Structural Determination of Biomolecular Interfaces by Nuclear Magnetic Resonance of Proteins with Reduced Proton Density – Supporting Information

Fabien Ferrage†, Kaushik Dutta, Alexander Shekhtman‡, David Cowburn*,

New York Structural Biology Center, 89 Convent Avenue, New York New York 10027 USA.

* Corresponding author: David Cowburn, New York Structural Biology Center, 89 Convent avenue, Park Building at 133rd St., New York, New York 10027, USA. Tel: 1 212 939 0660, cowburn@cowburnlab.org

† current address: CNRS – UMR 8642 and Ecole normale supérieure, département de chimie, 24, rue Lhomond, 75231 Paris Cedex 05, France.

‡ current address: State University of New York at Albany, 1400 Washington Ave., Albany, New York 12222, USA.

Contents

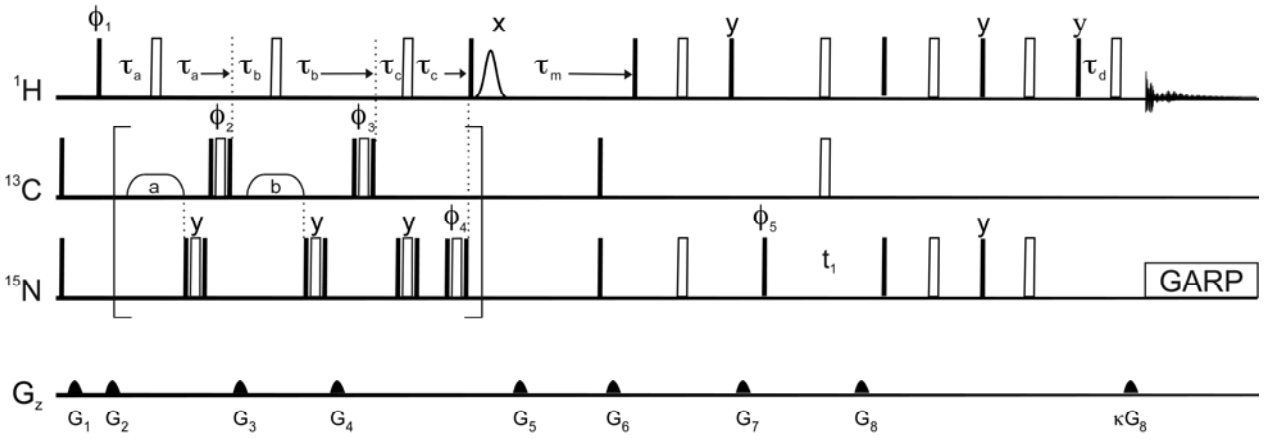

Figure S1: Pulse sequence for the detection of amide protons located at the biomolecular interface.

This sequence is very similar to the one published by Zwahlen et al..(Zwahlen, Legault et al. 1997) Readers should refer to the original article for details. Narrow filled and wide open rectangles are $\pi/2$ and π pulses, respectively. For convenience, dotted lines link events that are simultaneous and arrows indicate the end of the delays, if necessary. ^{13}C frequency shaped pulses are WURST adiabatic pulses(Kupce, Boyd et al. 1995) for B_0 = 16.4 T, with τ_{pa} = 2.36 ms and τ_{pb} = 1.53 ms. WURST pulses have a sweep amplitude of 70 kHz, they are on-resonance at 0 ppm at their half-duration. The maximum amplitude of WURST pulses is 5 kHz for the pulse of duration τ_{pa} = 2.36 and 6 kHz for the pulse of duration τ_{pb} = 1.53 ms pulse. Delays are: τ_a = 2.2 ms, τ_b = 2 ms and the delay τ_c is calculated as follows: $\tau_c = \tau - \tau_a - \tau_b + (\tau_{pa} + \tau_{pb})/2$, with $\tau = |4J_{NH}|^{-1}$ = 2.7 ms where J_{NH} is the NH scalar-coupling constant. The τ_m delay is the cross-relaxation mixing time. The short delay τ_d compensates for chemical shift evolution during the last gradient κG_8. To suppress the effect of cross-relaxation or exchange with the solvent in experiments, a 1.41 ms Gaussian $\pi/2$ pulse may be inserted at the beginning of the mixing time τ_m. The ^{13}C carrier is positioned at 110 ppm for the initial purging pulse as well as for the decoupling pulse during the

t_1 evolution and it was set to 27 ppm for rest of the experiment. During the filter section, gradients strengths are set such that: $G_2 + G_4 = G_3$. For echo-antiecho phase selection, the gradient ratio is $\kappa = 0.101$. Sensitivity-enhancement was performed with a PEP scheme. The phase cycle was: $\phi_1 = 8\{x,x,-x,-x\}$; $\phi_2 = 4\{4\{y\},4\{-x\}\}$; $\phi_3 = 2\{8\{y\},8\{-x\}\}$; $\phi_4 = 16\{y\},16\{-x\}$; $\phi_5 = 16\{x,-x\}$ and $\phi_{acq} = 8\{x,-x,-x,x\}$. For the experiment with no filter, the pulses within parenthesis are suppressed. For the experiment where filter section is deleted, transverse relaxation of the protons has to be taken into account in the analysis of the normalized polarization transfer using the empirical relationship: $R_2/\tau_c = 5.10^9$ s^{-2}. In the case of fast exchange, the average correlation time of the source protein between the bound and free forms should be used. In the case of slow exchange, the overall tumbling time should be used. A rigorous treatment of intermediate cases would require the use of a more complete model such as the one employed in the CORCEMA protocol.(Jayalakshmi and Krishna 2002) Note that it is possible to evaluate the transverse relaxation rate of the HIPRO partner in a 1:1 echo experiment (Sklenar and Bax 1987) preceded by an isotope filter.

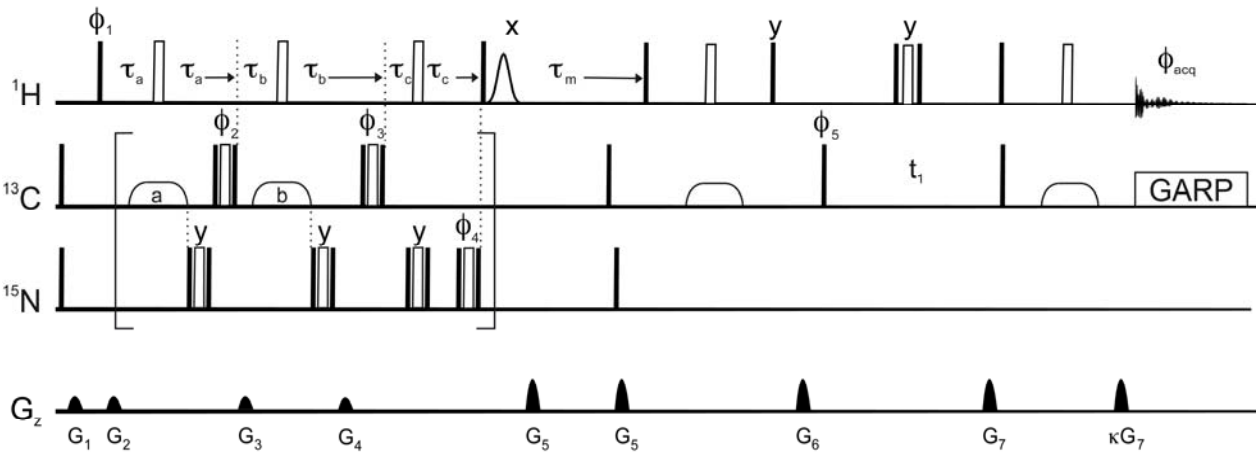

Figure S2. Pulse sequence of the $^{1}H\{^{13}C\}$ HSQC-edited filtered NOESY.

This pulse sequence is very similar to Figure S-1. All the differences are discussed below. To suppress the effect of residual polarization from the solvent, a 1.41 ms Gaussian $\pi/2$ pulse followed by a pulses field gradient were inserted at the beginning of the mixing time τ_m. The duration of the delay τ is 1.85 ms. The inversion of ^{13}C in the HSQC part of the above pulse sequence is done by using 500 μs smoothed CHIRP (frequency sweep: 60 kHz) pulses(Bohlen and Bodenhausen 1993) for the Csk SH3-PEP complex and by using 256 μs Q3 pulses{Emsley, 1990 #61} for the ubiquitin-AUIM complex, respectively. For the Csk SH3-PEP complex, ^{13}C carrier frequency was set to 37.5 ppm and 120 ppm, respectively, when acquiring the $^{1}H\{^{13}C\}$ HSQC-edited filtered NOESY experiment for the aliphatic and aromatic region. The gradient ratio κ is 0.25. Pulses on the ^{15}N channel were deleted for the experiments with the Csk-SH3-PEP complex.

Figure S3. Spectra obtained by using the filtered NOESY experiments (Figs. S1 and S2).

Positive and negative contour levels are shown in black and red respectively. The series consists of groups of three spectra: the first two are interleaved filtered-NOESY experiments obtained with 1 ms (first spectrum) and 300 ms (second spectrum) mixing times; the third spectrum is the REDSPRINT spectrum, obtained by subtracting the first one from the second one, as described in the text. In each group of three spectra, the contour levels are identical. The **ubiquitin-AUIM sample**: (a-c) $^{1}H\{^{15}N\}$ HSQC-edited filtered NOESY spectra; (d-f) $^{1}H\{^{13}C\}$ HSQC-edited filtered NOESY spectra. The **Csk SH3-PEP sample in $^{2}H_2O$**: (g-i) $^{1}H\{^{13}C\}$ HSQC-edited filtered NOESY spectra edited in the aromatic region; (j-l) $^{1}H\{^{13}C\}$ HSQC-edited filtered NOESY spectra edited in the aliphatic region. **Csk SH3-PEP sample in $^{2}H_2O$/ [$^{2}H_8$] glycerol**: (m-o) $^{1}H\{^{13}C\}$ HSQC-edited filtered NOESY spectra edited in the aliphatic region.

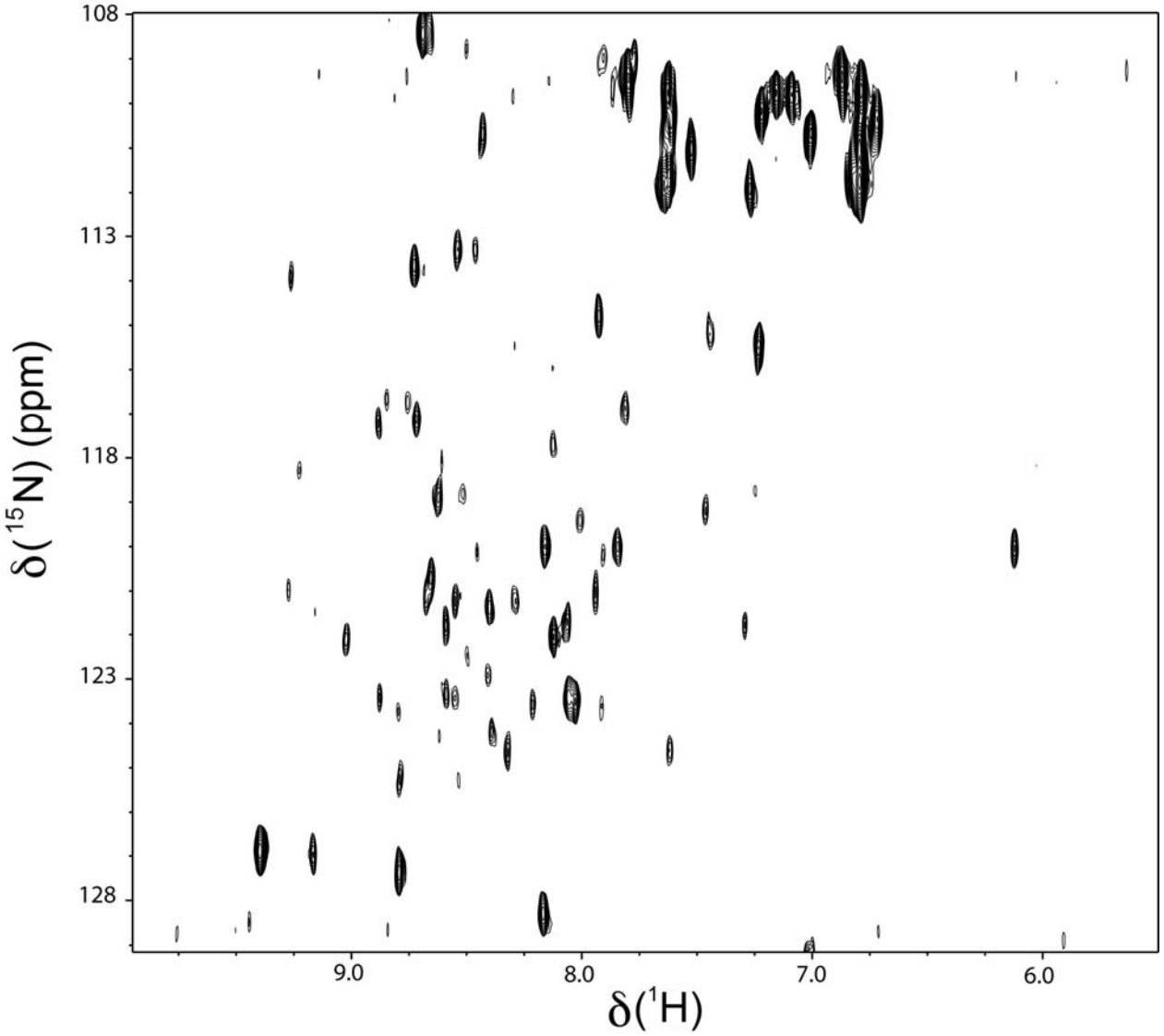

Figure S3a

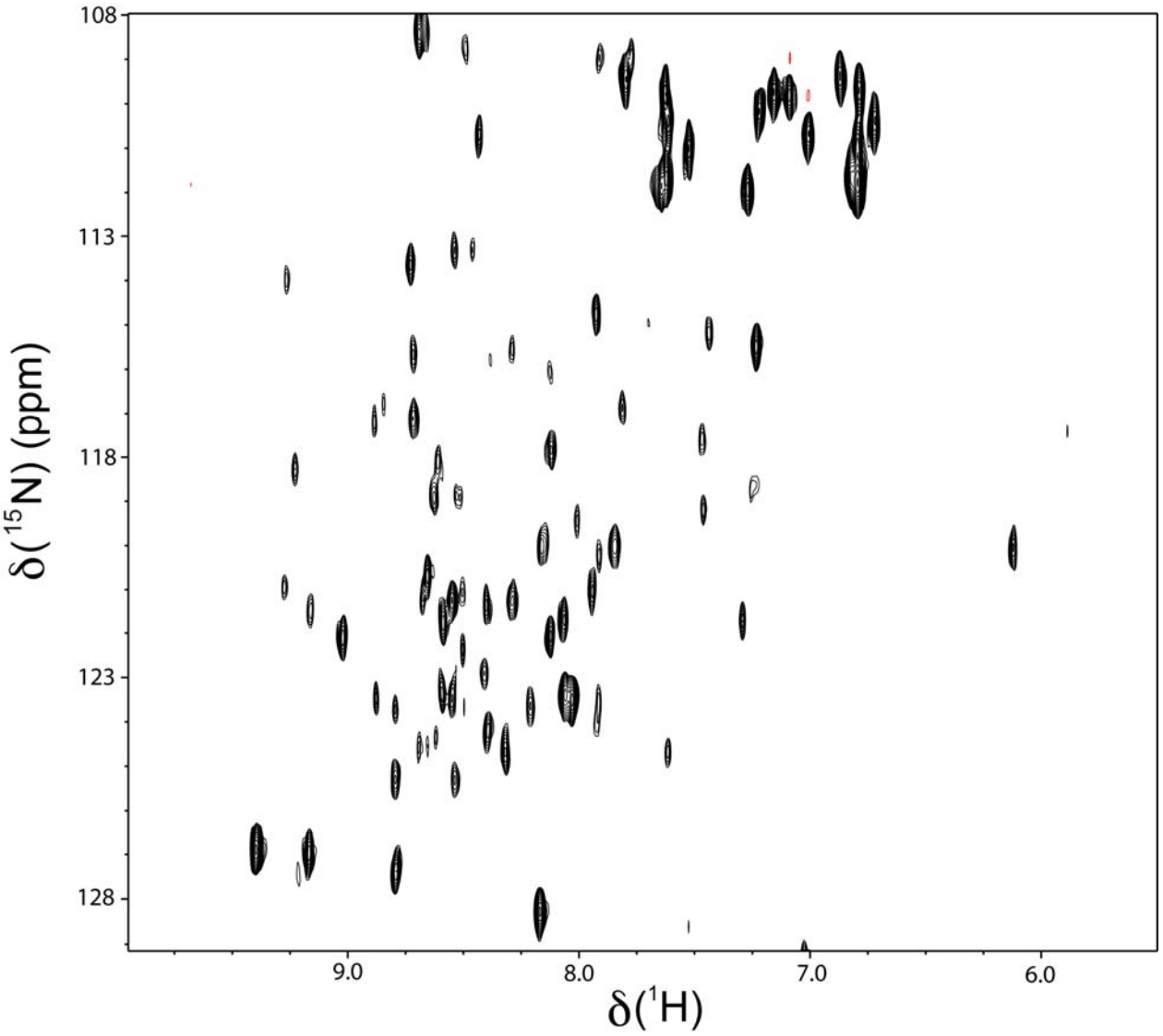

Figure S3b

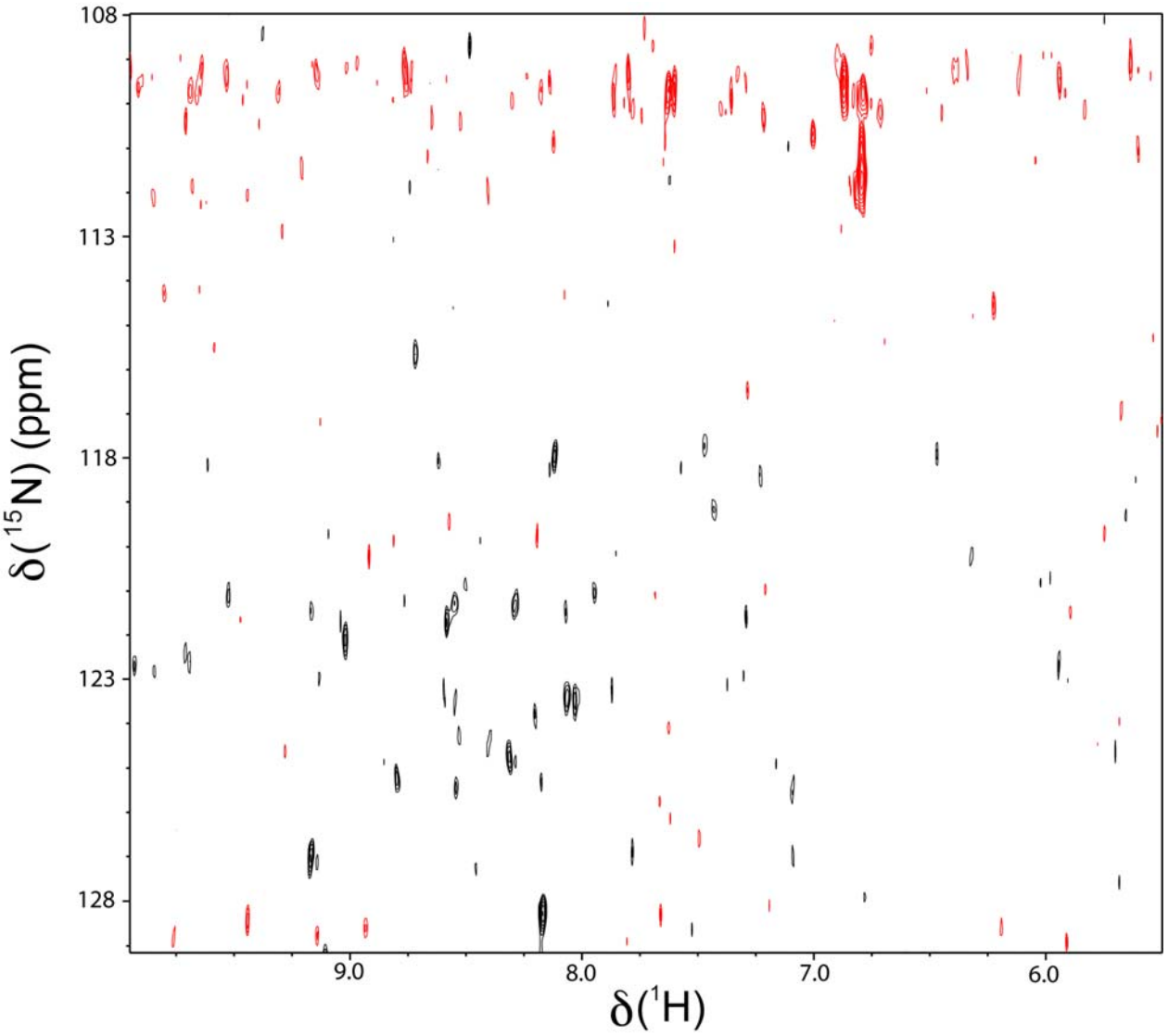

Figure S3c

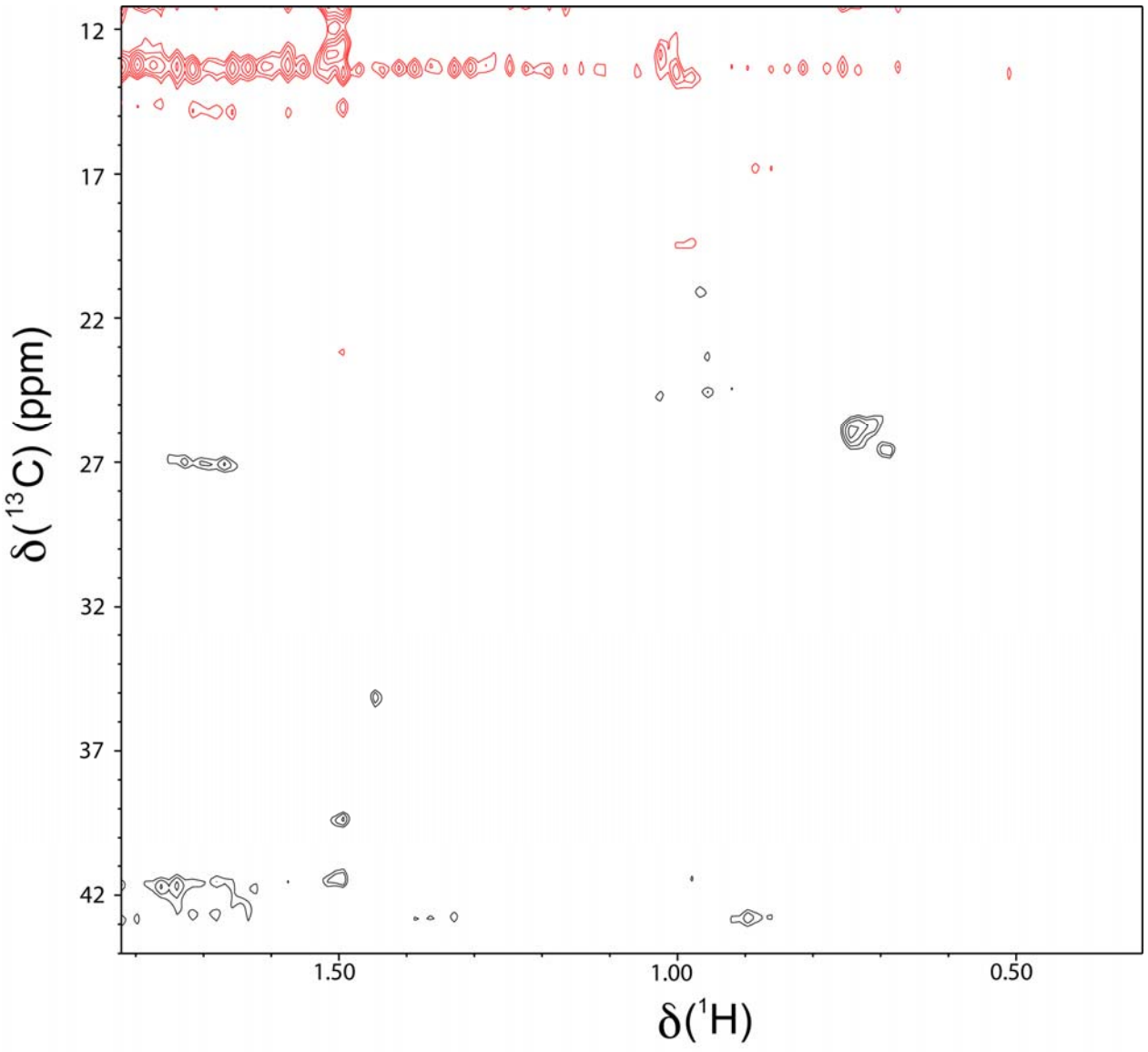

Figure S3d

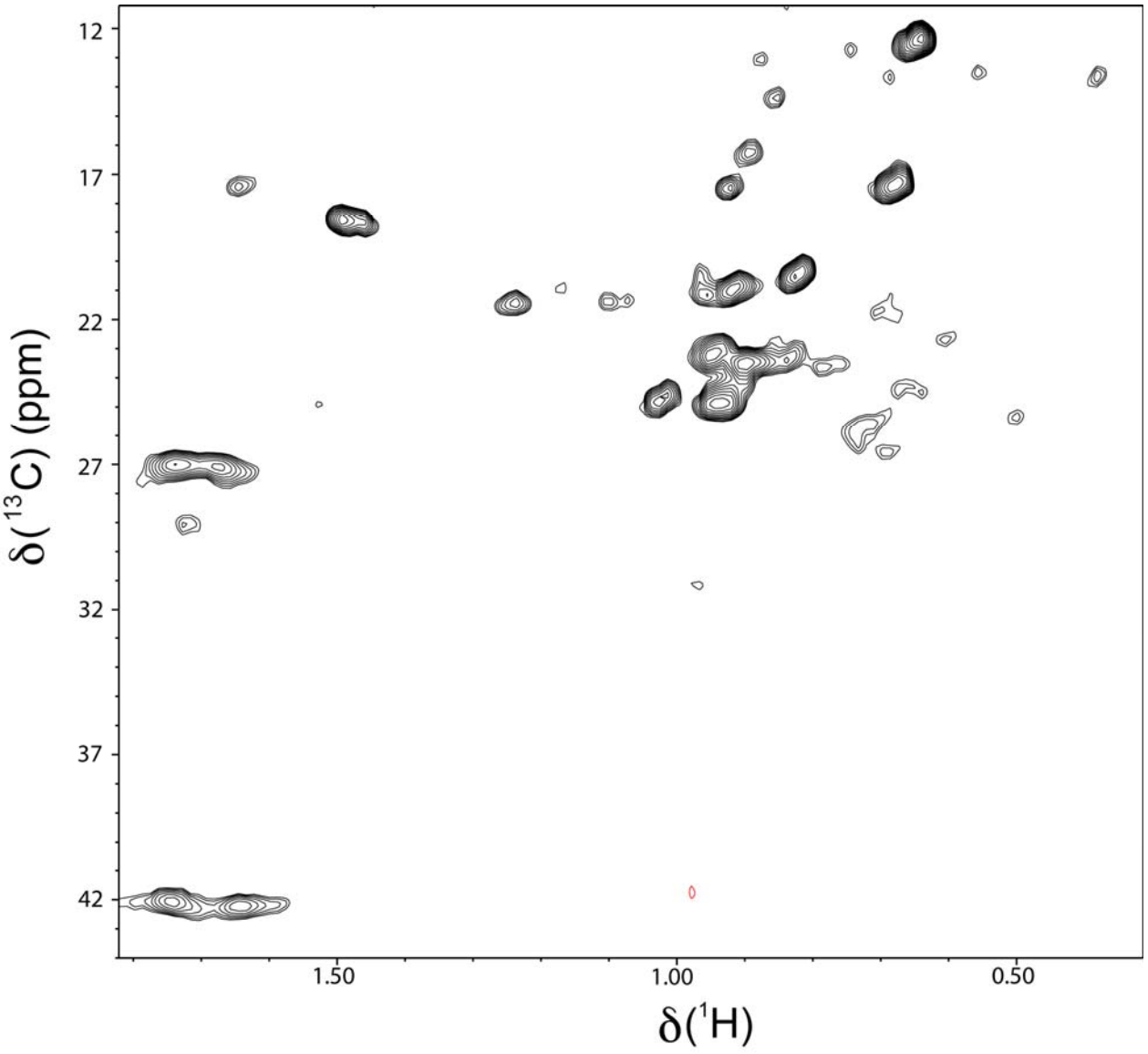

Figure S3e

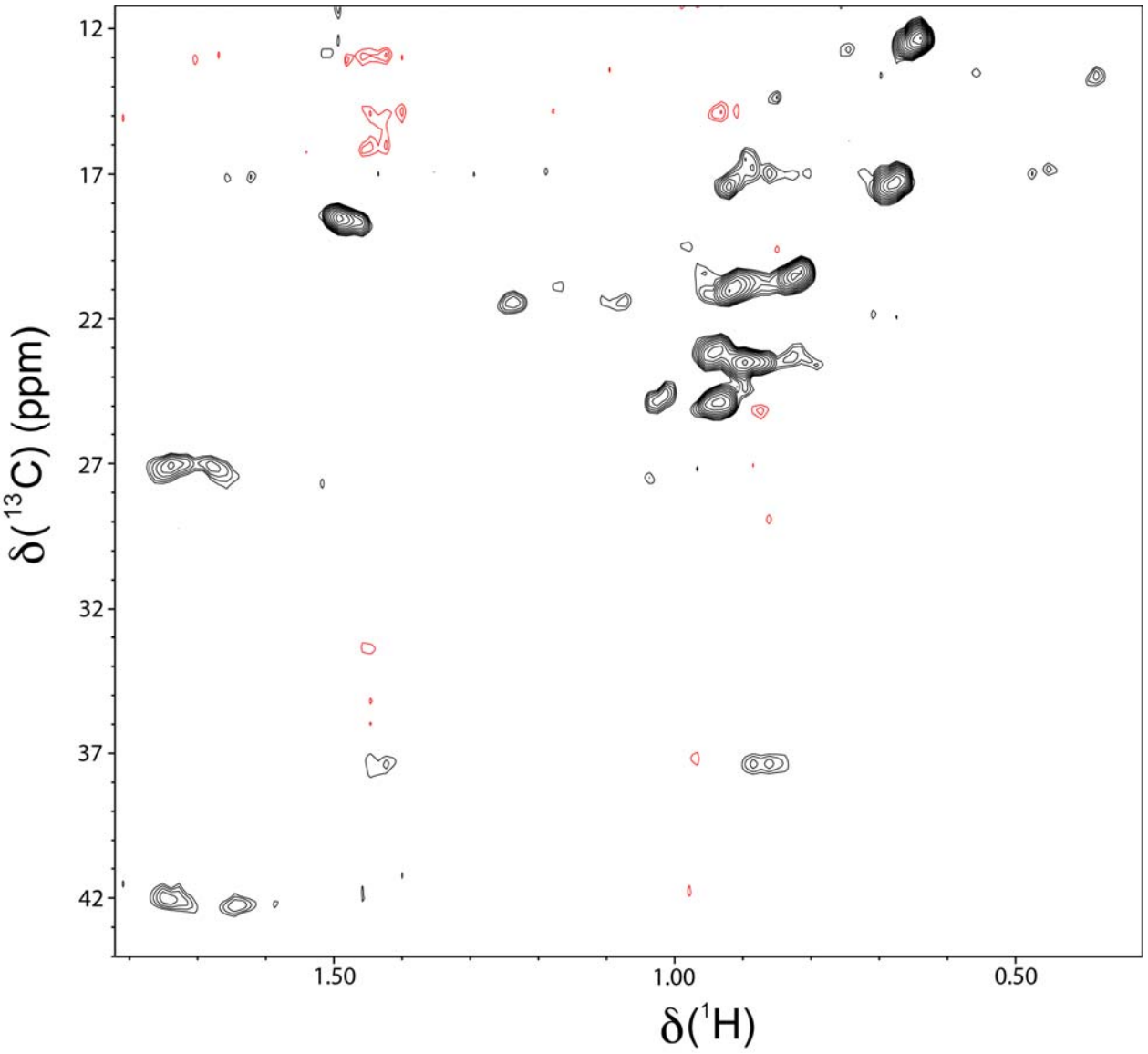

Figure S3f

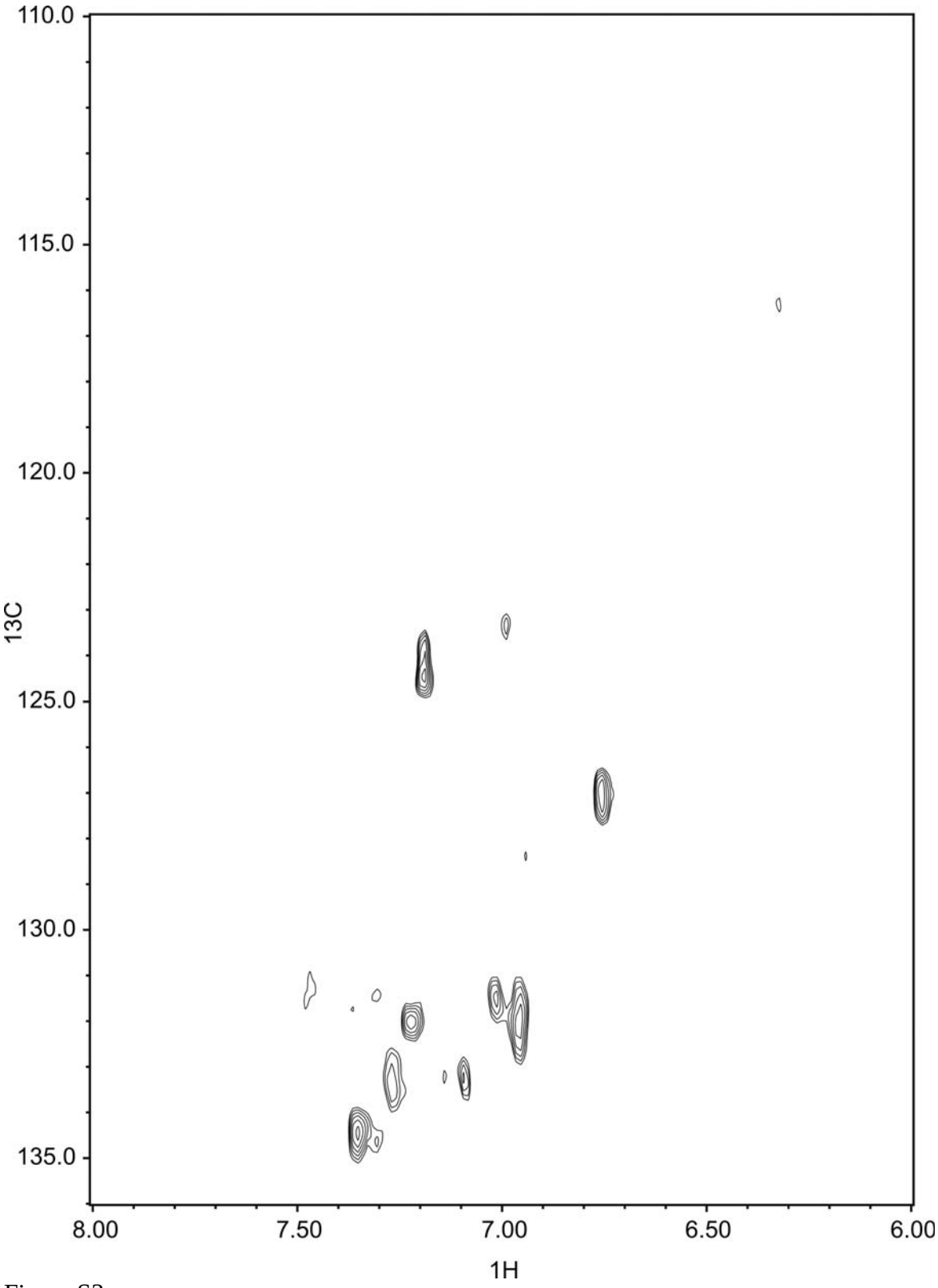

Figure S3g

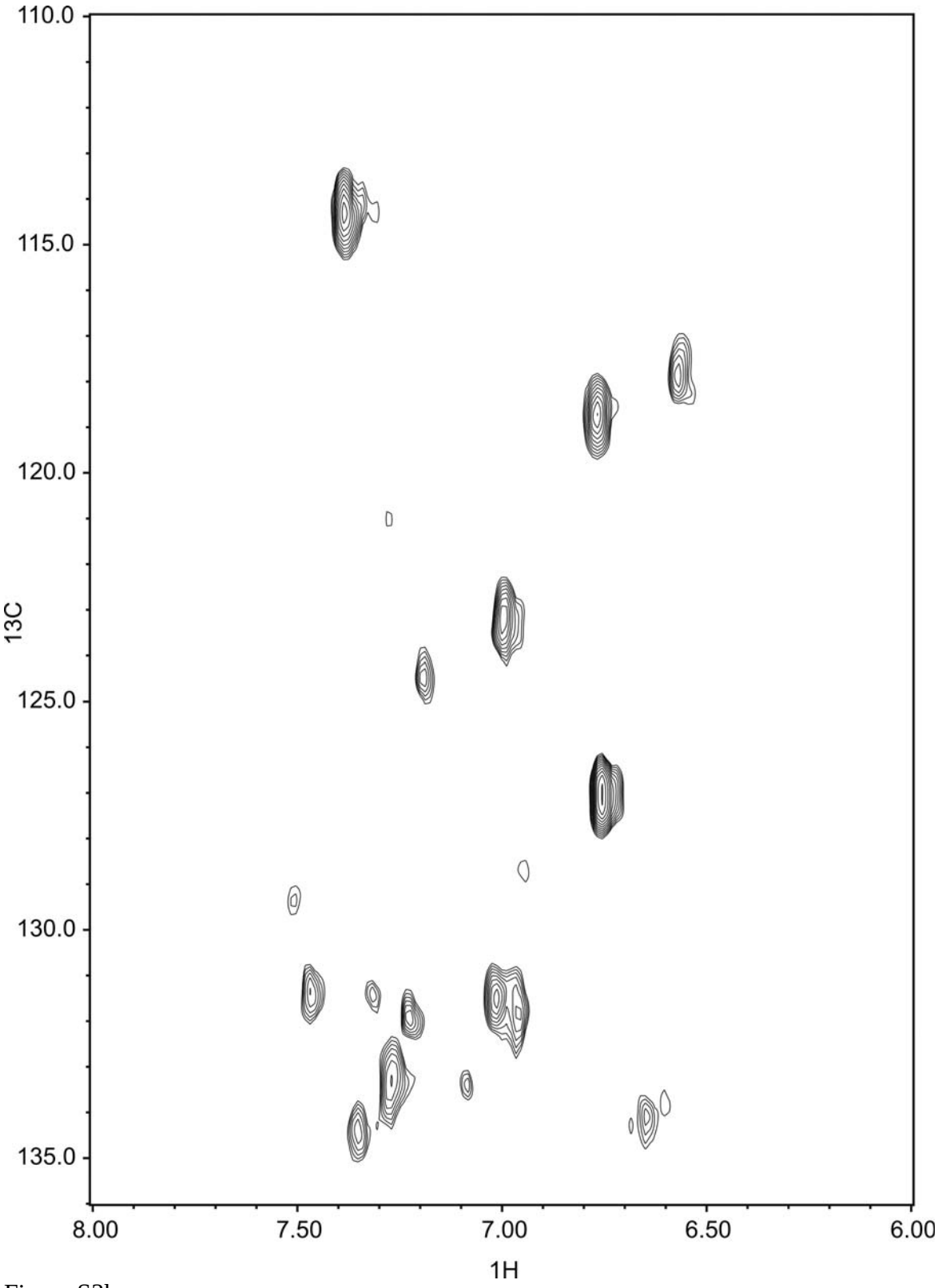

Figure S3h

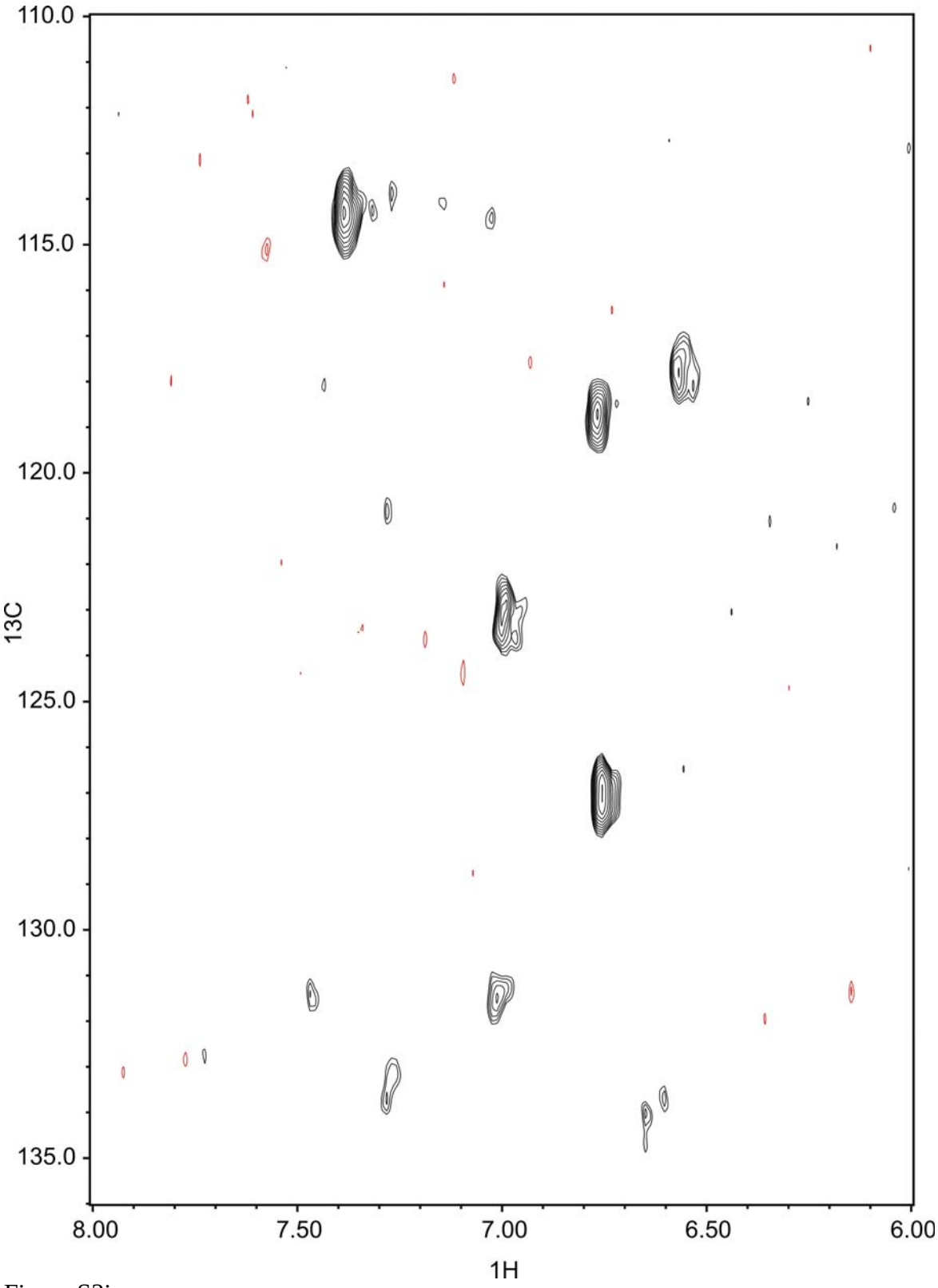

Figure S3i

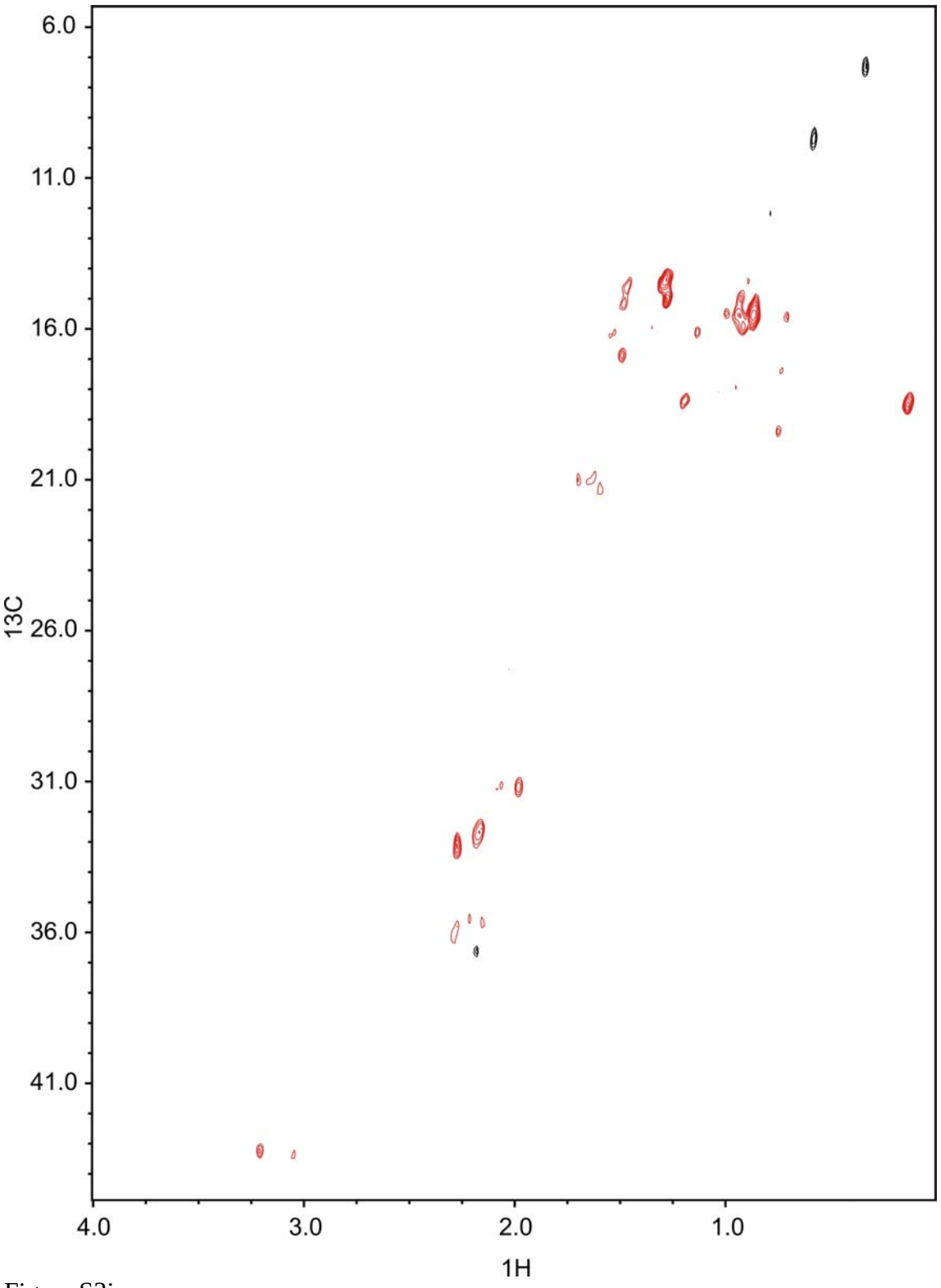

Figure S3j

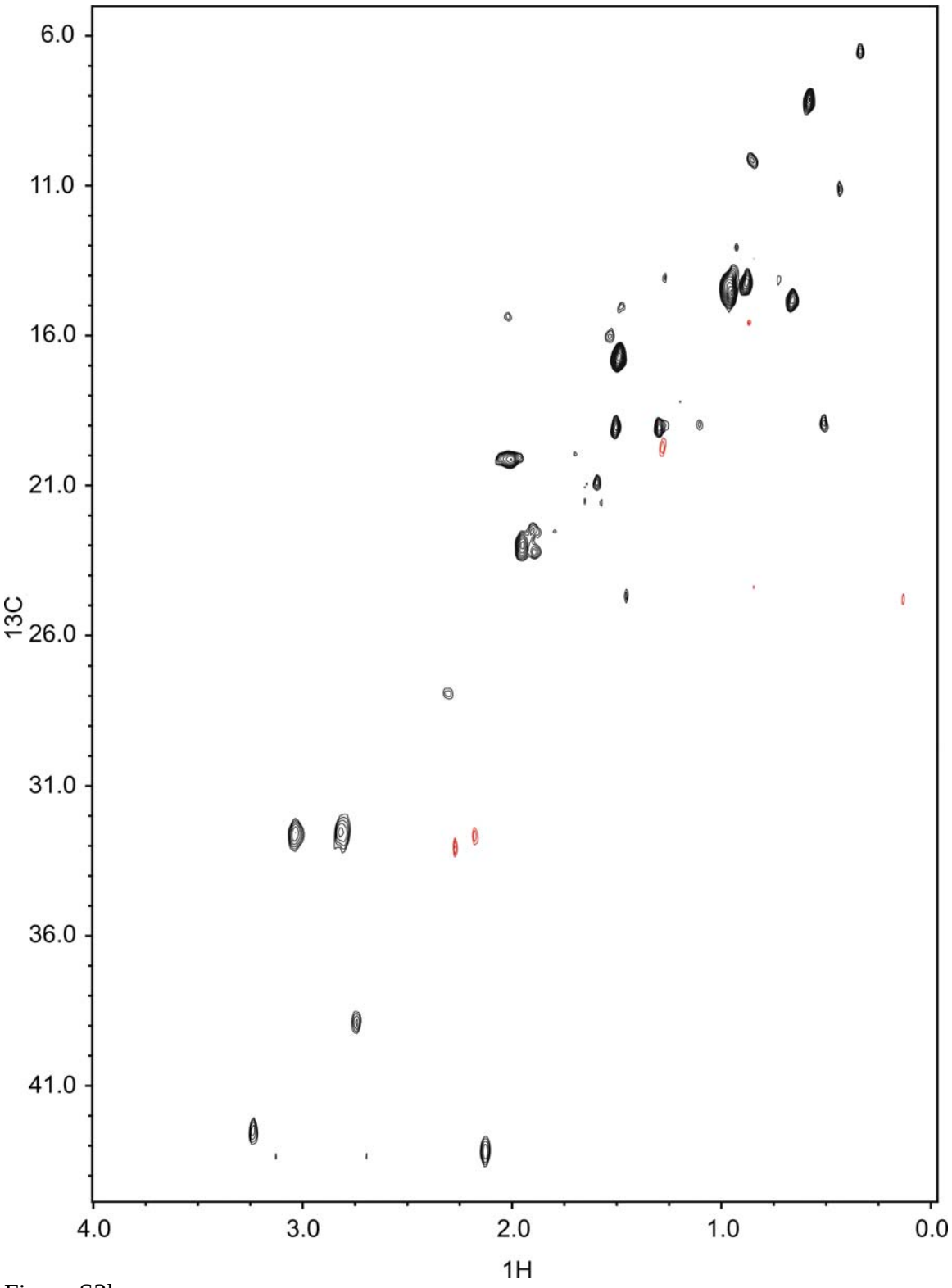

Figure S3k

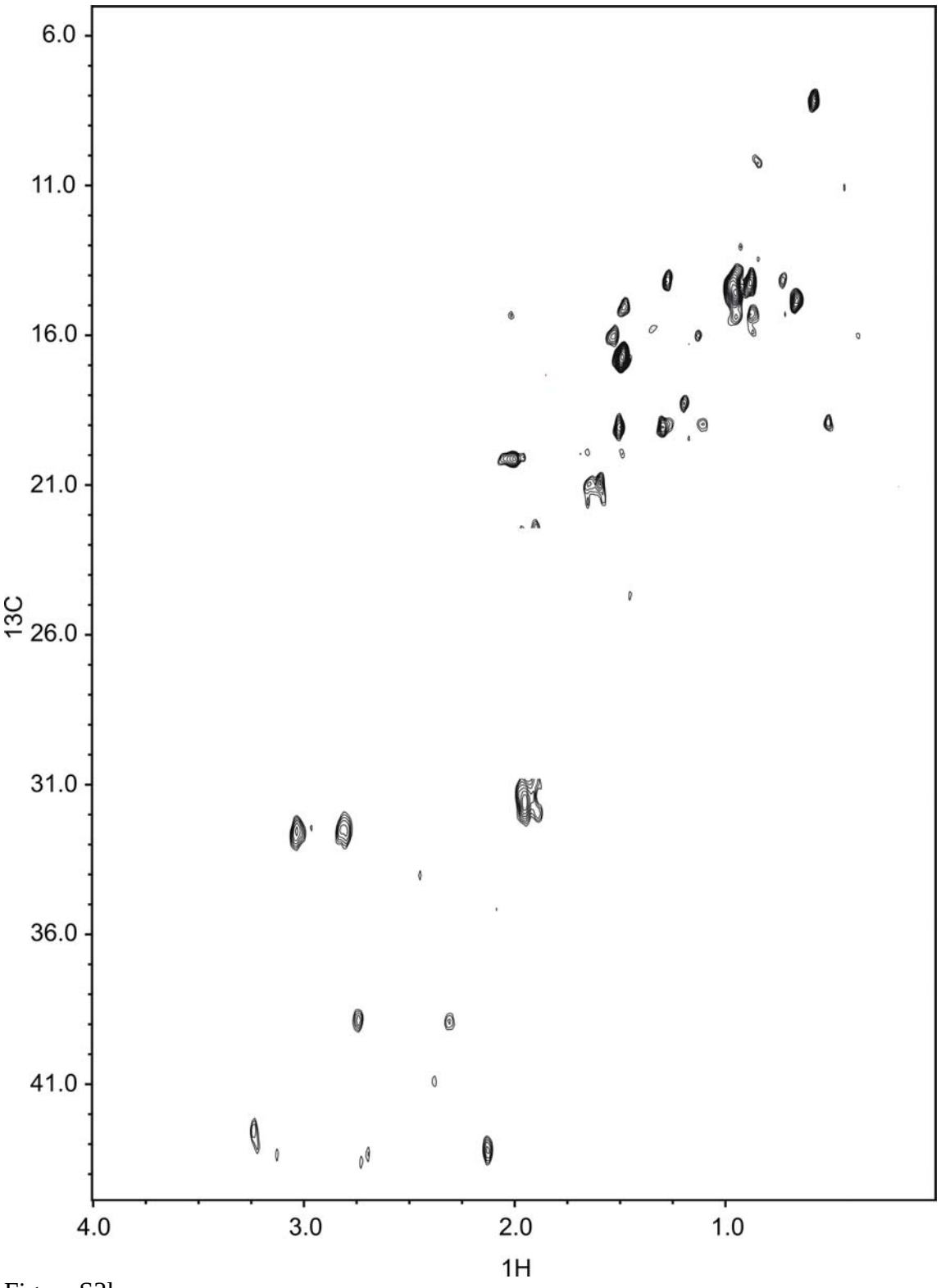

Figure S3l

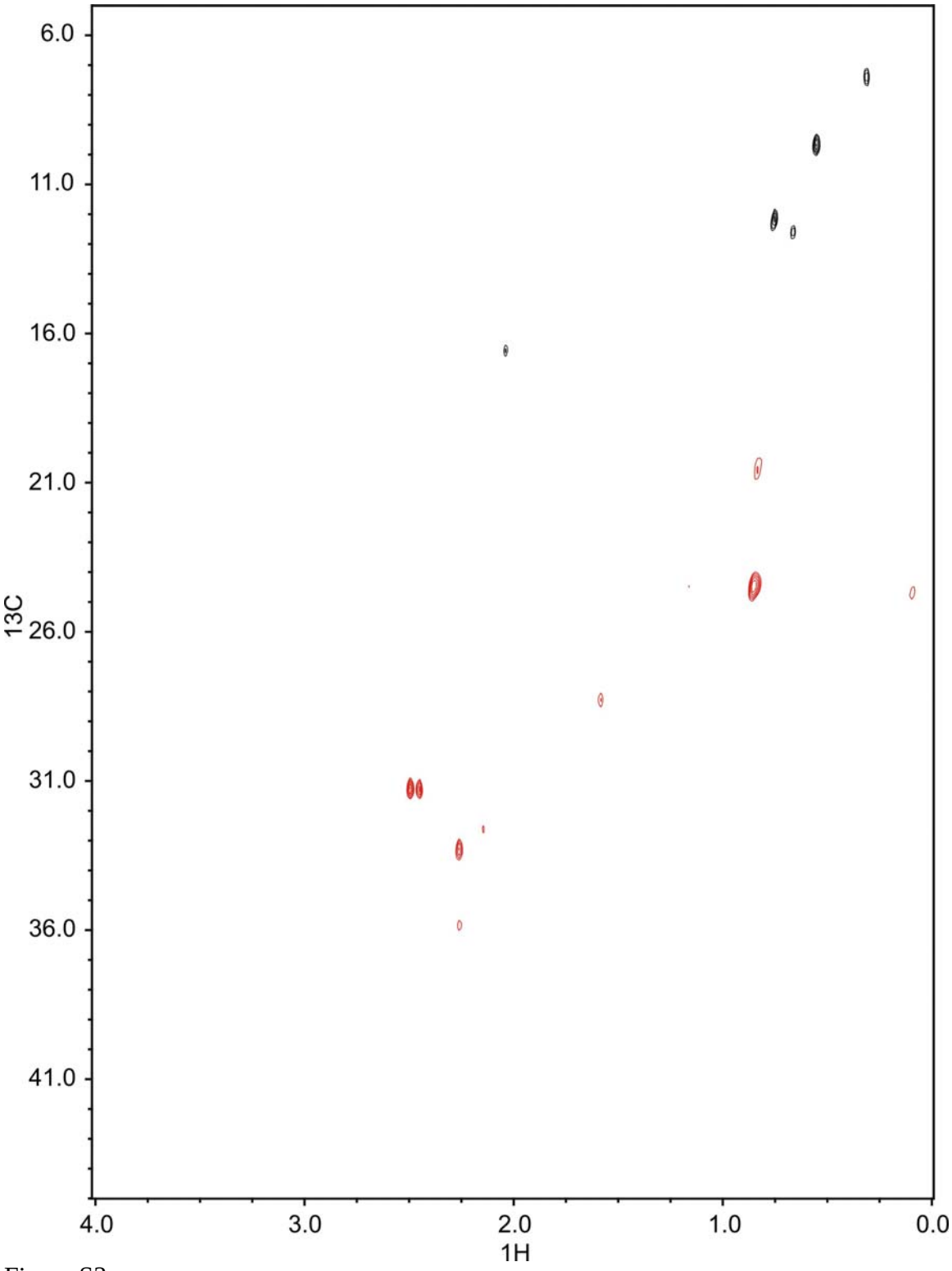

Figure S3m

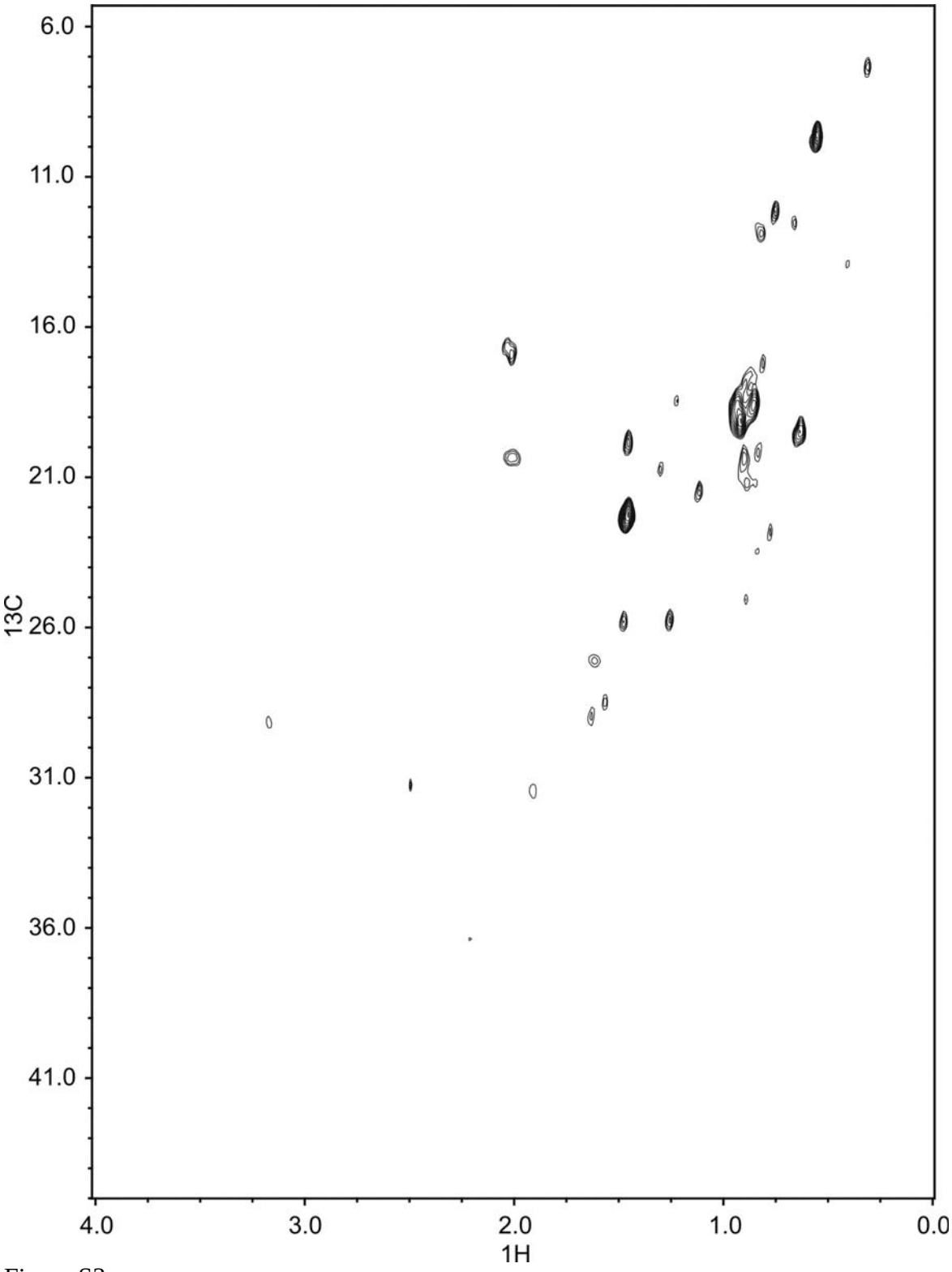

Figure S3n

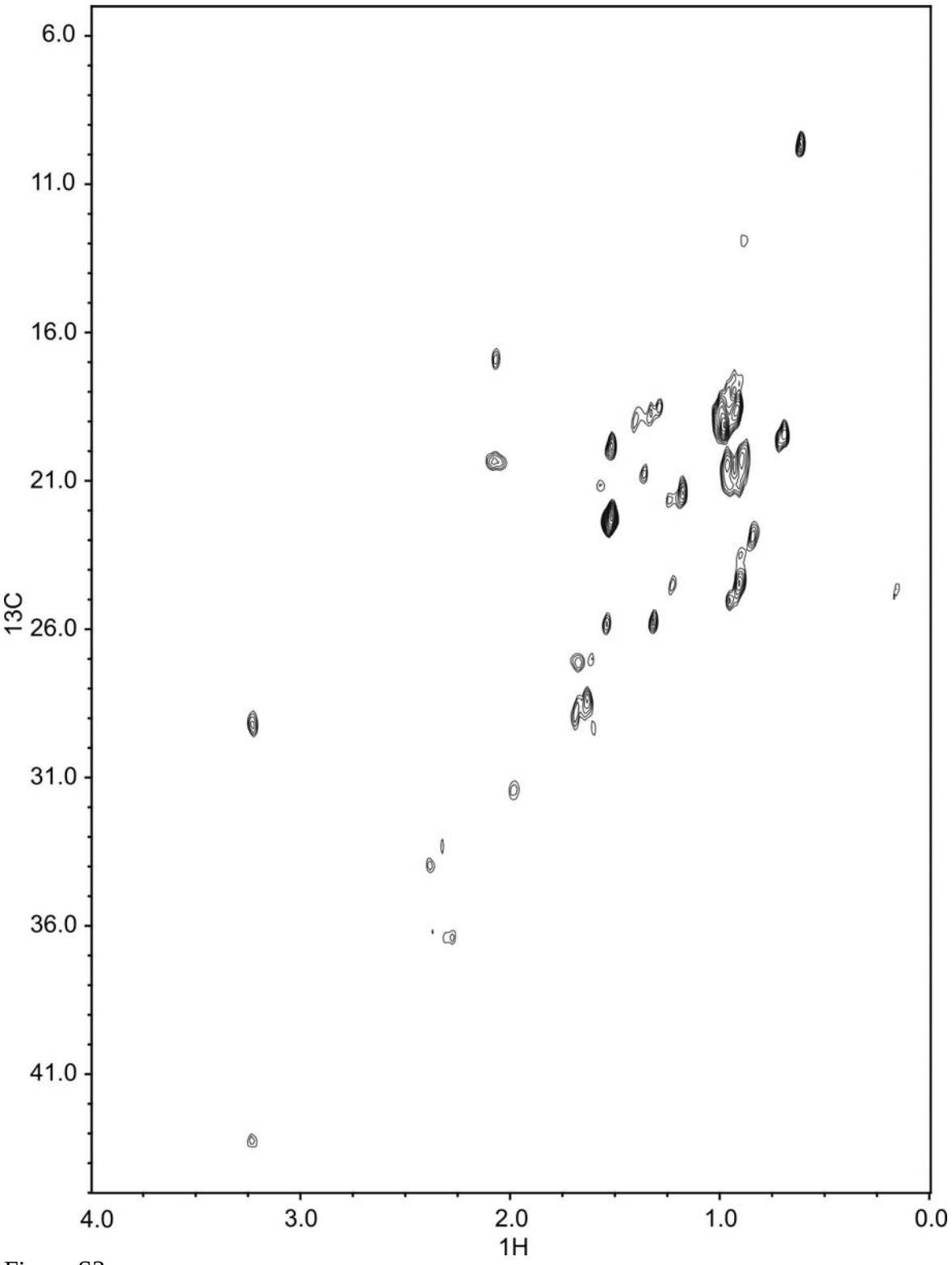

Figure S3o

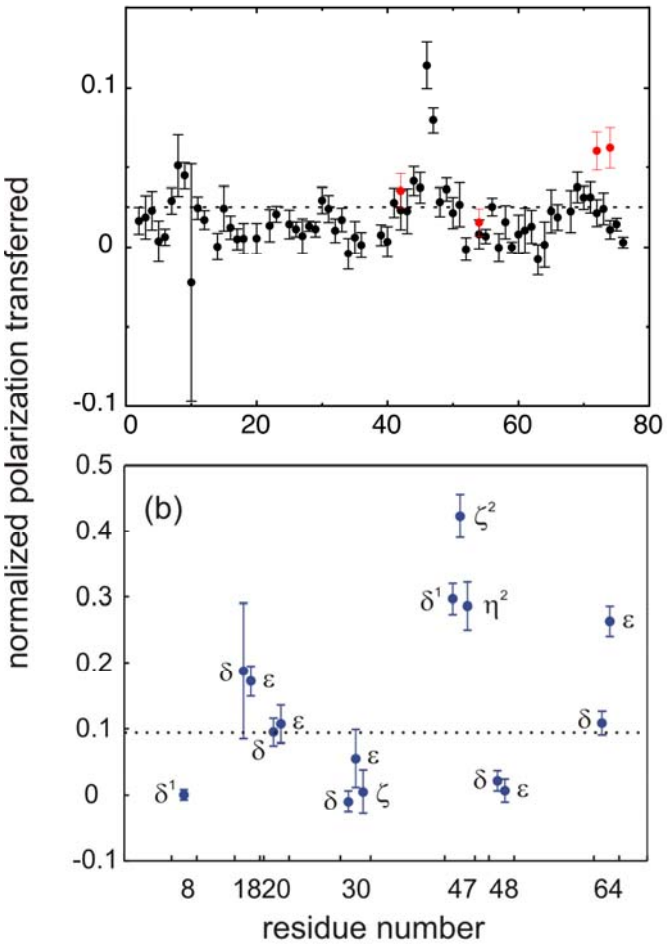

Figure S4. Normalized polarization transfer (eq. 8, text) for (a) amide protons of ubiquitin in the ubiquitin-AUIM complex and (b) the aromatic side-chain protons of the Csk SH3-PEP complex.

Black and red circles represent backbone amides and arginine side-chain ε protons respectively. (b) The aromatic side-chain protons of the Csk SH3-PEP complex. Assignments are provided next to each point. Dotted lines represent the threshold over which restraints were identified. The threshold is typically chosen close to 20% of the maximum value. The values are computed according to Eq. 8.

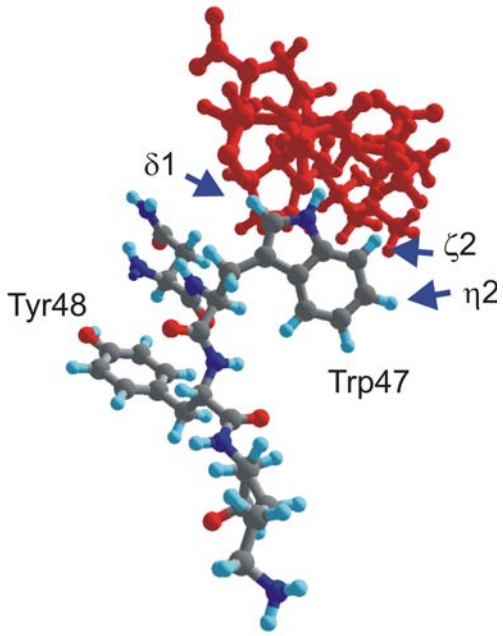

Figure S5. Expanded view of the structure of the Csk SH3-PEP complex, to illustrate the atomic resolution of REDSPRINT constraints.

The side-chain of residue Trp47 is located at the interface. Only hydrogen atoms in direct contact with PEP (red) show a significant polarization transfer (see Fig. S4b). The side-chain of Tyr48 (the next residue), which is buried inside the Csk SH3 domain, does not show any polarization transfer from the PEP ligand. (see Fig. S4b).

Table S1. Normalized polarization transfer ratios for the Csk SH3 side-chain ^{13}C-bound protons in the complex with the PEP in $^{2}H_2O$ (threshold 0.15):

Proton	Normalized polarization transfer ratio	Error*
8.HD1	0.001	0.013
16.HB1	0.126	0.010
18.HB2	0.773	0.113
18.HD	0.298	0.163
18.HE	0.274	0.036
19.HB2	0.294	0.034
20.HD	0.151	0.033
20.HE	0.170	0.045
23.HG21	0.052	0.005
24.HB1	0.132	0.010
30.HD	-0.015	0.026
30.HE	0.088	0.069
30.HZ	0.008	0.053
40.HB1	0.231	0.005
41.HG22	0.100	0.005
43.HB1	0.271	0.017
43.HD1	0.097	0.009
46.HB2	0.800	0.151
47.HB1	0.373	0.038
47.HB2	0.430	0.050
47.HD1	0.472	0.037
47.HN2	0.454	0.057
47.HZ2	0.672	0.052
48.HD	0.035	0.024
48.HE	0.011	0.028
49.HG1	0.281	0.021
49.HG2	0.389	0.026

59.HD11	0.092	0.008
59.HG21	0.210	0.007
62.HB1	0.044	0.002
64.HD1	0.172	0.029
64.HE	0.419	0.036

*The error in the peak intensity was considered to be equal to the noise. It was then propagated along the computation of the normalized polarization transfer.

Table S2. Normalized polarization transfer ratios above the threshold for the Csk SH3 side-chain ^{13}C-bound protons in the complex with the PEP in the $^{2}H_2O$/glycerol mixture (threshold 0.15):

Proton	Normalized polarization transfer	Error*
16.HB1	0.182	0.023
18.HB1	0.516	0.111
18.HE	0.426	0.132
24.HB1	0.173	0.010
40.HB1	0.360	0.009
41.HG11	0.163	0.007
41.HG22	0.182	0.009
42.HG21	0.296	0.009
43.HB1	0.373	0.051
43.HG1	0.481	0.046
43.HG2	0.390	0.030
47.HB1	0.564	0.153
47.HB2	0.678	0.201
47.HD1	0.251	0.143
47.HN2	0.521	0.258
47.HZ2	0.742	0.200
59.HD11	0.204	0.010
64.HE	0.242	0.120

Table S3. Intermolecular correlations detected in an isotope-filtered NOESY spectrum of a HIPRO sample of ubiquitin in complex with AUIM:

assignment	$\delta(^{13}C)$	assignment	$\delta(^{1}H)$ Ubiquitin	$\delta(^{1}H)$ AUIM	intensity
5.CG1	20.09012	5.HG1	0.69755	0.65775	0.6624
8.CD1	24.65942	8.HD1	1.01620	2.77846	0.7972
8.CD1	24.61036	8.HD1	1.01516	1.90157	0.5666
8.CD2	23.21183	8.HD2	0.94061	1.67159	0.4510
8.CD2	23.16638	8.HD2	0.93863	1.45616	0.7064
8.CD2	23.21796	8.HD2	0.93918	0.86324	2.5208
13.CD1	13.65826	13.HD1	0.69003	0.75593	0.3382
13.CG2	17.08134	13.HG2	0.83980	0.74254	0.6995
17.CG2	18.83284	17.HG2	0.39831	0.72190	0.4127
30.CD1	14.57487	30.HD1	0.85724	0.72573	0.9402
44.CG1	27.41667	44.HG11	1.03904	0.84824	0.3167
44.CG1	27.38465	44.HG12	1.29398	0.84327	0.3573
44.CG2	17.08081	44.HG2	0.65901	3.91569	1.1221
44.CG2	17.10034	44.HG2	0.65826	1.69265	0.5311
44.CG2	16.98592	44.HG2	0.65835	1.45966	0.7156
44.CG2	17.00064	44.HG2	0.65861	0.81966	2.2708
44.CG2	16.86290	44.HG2	0.65904	0.61535	0.5244
43.CD1	25.98235	43.HD1	0.72412	0.46151	0.3518
44.CD1	12.33841	44.HD1	0.64494	1.67671	0.6958
44.CD1	12.33349	44.HD1	0.64459	1.45805	1.3377
44.CD1	12.33400	44.HD1	0.64479	0.87426	2.7046
46.CB	15.91786	46.HB	0.87045	0.85172	0.9848
61.CD1	13.71624	61.HD1	0.37973	0.50497	0.4225
61.CG2	16.59729	61.HG2	0.44075	0.61152	0.4419
70.CG1	20.32040	70.HG1	0.80804	2.79532	0.3290
70.CG1	20.31201	70.HG1	0.80621	1.67433	0.3852
70.CG1	20.26098	70.HG1	0.80683	1.44955	2.3738
70.CG2	20.80083	70.HG2	0.90621	1.69155	0.5088
70.CG2	20.80654	70.HG2	0.90301	1.45310	0.8557
70.CG2	20.73744	70.HG2	0.90333	0.84663	1.5769
73.CD2	22.84940	73.HD2	0.84285	1.63875	0.3031

The total duration of the 3D NOESY was as long as the two ^{13}C-edited REDSPRINT spectra.

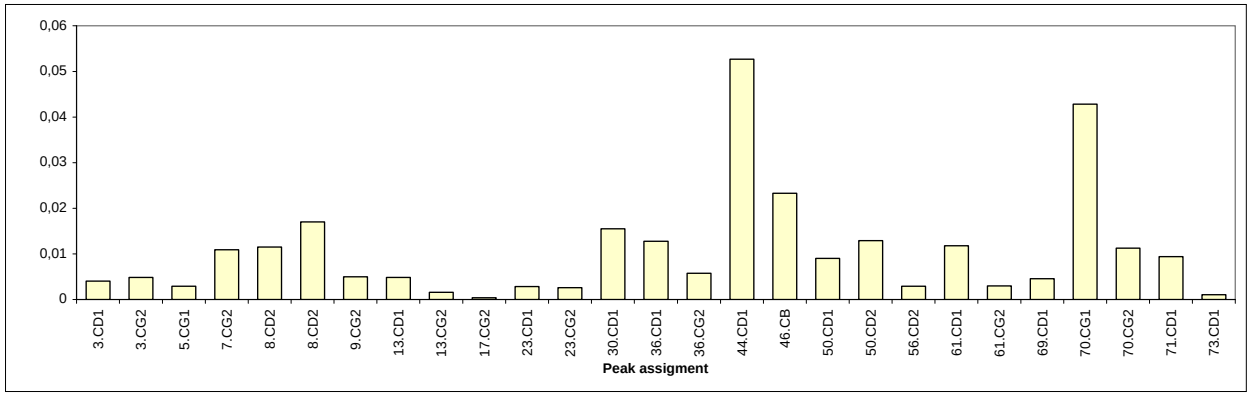

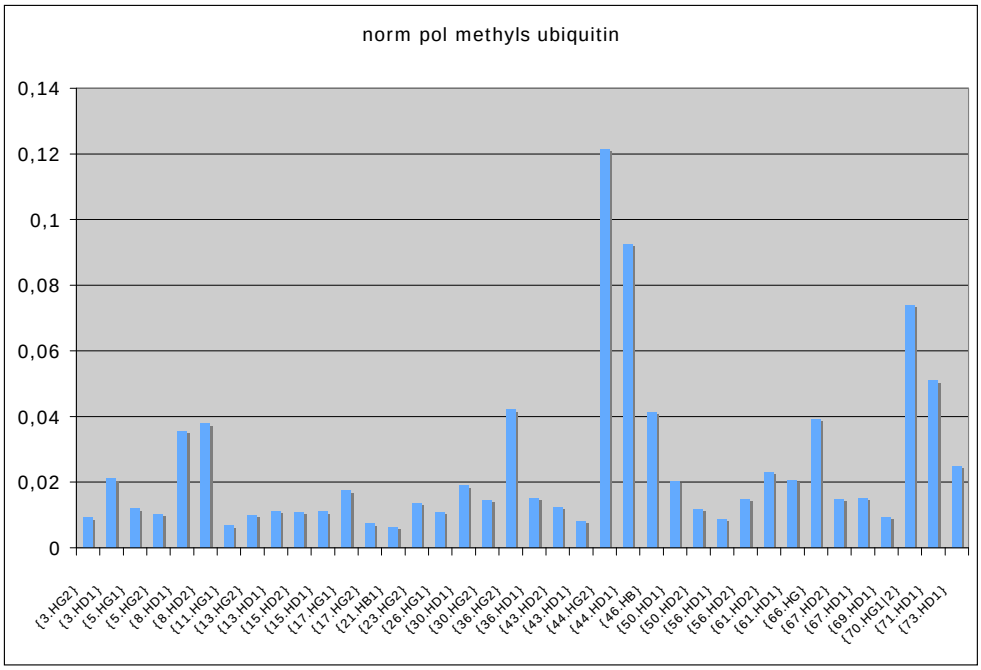

Figure S6. Chemical shift perturbations for the methyl groups of ubiquitin upon binding of AUIM.

The apo and holo $^{1}H\{^{13}C\}$ HSQC spectra were recorded on a sample of [^{15}N, ^{13}C] labeled ubiquitin with and without AUIM. The chemical shift perturbation was computed from the variations of ^{1}H and ^{13}C chemical shifts of individual signals, $\Delta\delta(^{1}H)$ and $\Delta\delta(^{13}C)$ respectively,

according to the following expression: $\left(\left[\Delta\delta\left({}^{1}\mathrm{H}\right)\right]^{2}+\left[\Delta\delta\left({}^{13}\mathrm{C}\right)/10\right]^{2}\right)^{1/2}$. ^{13}C Chemical shift variations were scaled down by an unusually small factor 0.1 in order to enhance the sensitivity of the above-mentioned expression to ^{1}H chemical shift variations (the standard deviation for ^{13}C shift changes is 30 times larger than that for ^{1}H) With a low threshold at 0.01, one can identify methyl groups of the hydrophobic patch (Leu8, Ile44 and Val70) as well as a few neighboring residues (Thr7, Leu71), in addition to some residues at the edges of a typical ubiquitin-UIM interface, such as Ile36 and Ile61. On the other hand, Ile30 and Ile50 show a measurable chemical shift perturbation even though they are not exposed at the surface of ubiquitin.

Theoretical comparison of REDSPRINT with other methods for the detection of transient intermolecular effects:

The following simulations were carried out on the same system that produced the data presented in Figure 2 (main text). In the first set of simulations, the efficiency of the polarization transfer using a fully protonated target system was computed. Results are shown in Figure S7.

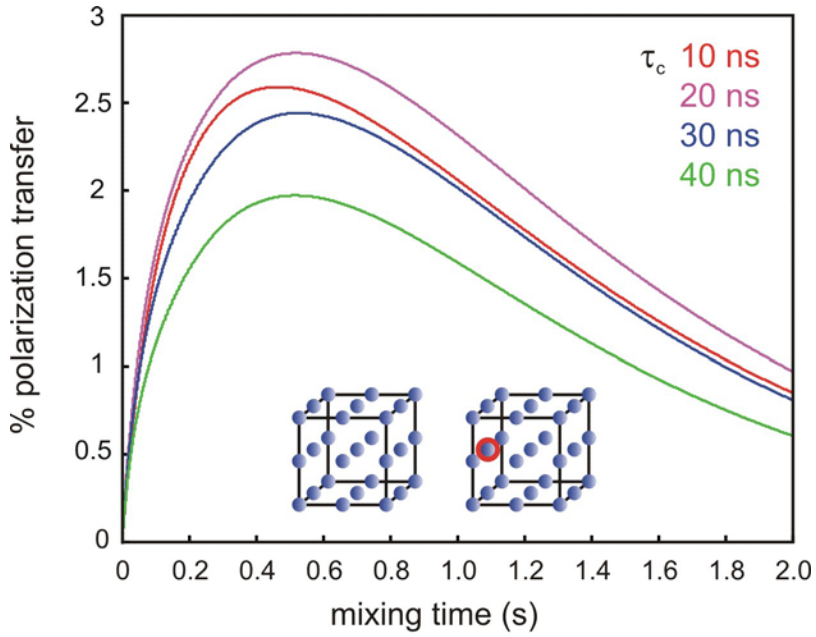

Figure S7: Simulations of the polarization transfer efficiency with a HIPRO target.

This figure is similar to Figure 2 of main text. The transfer from the left-side cube to the sphere circled in red in the right-side cube is plotted versus the duration of the transfer. The difference between this figure and Figure 2 is that the occupancy for ^{1}H on the right hand side cube illustrated is changed from 0.1 to 1.0, i.e. fully protonated (HIPRO).

The efficiency of transfer expected after a 300 ms mixing time is between 2 and 2.5 % for systems up to a 30 ns tumbling time. This compares with the 4 to 5 % efficiency in REDSPRINT. If one takes into account a ten-fold increase in the proton population, this amounts to a five-fold increase in sensitivity compared to REDSPRINT. However, the sensitivity of the HSQC part of the sequence is not taken into account. Protonation of the ^{13}C-labeled target protein leads approximately to a two-fold increase in the transverse relaxation rates of the protons. This leads to a decrease of the efficiency of the INEPT transfers and an increase of the peak line-width in the proton dimension. For a ^{13}C-bound proton in a 20 ns tumbling-time system, the difference in proton transverse relaxation rates in a HIPRO and a REDPRO sample can be estimated to be $\Delta R_2 = 90\ s^{-1}$; with an INEPT transfer delay $\tau = 1.85$ ms (see Fig. S2). The relative loss of efficiency is therefore: $\exp(-4\Delta R_2\tau) = 0.51$.

In addition, the proton line-width is expected to increase by a factor of two, so that the intensity of a given peak in an HSQC spectrum is expected to be decreased by a factor of four in a HIPRO protein as compared to a REDPRO protein. As a consequence, the use of a REDPRO target protein will lead to an increase in sensitivity for complexes with a tumbling time larger than 20 ns.

To evaluate the influence of the level of deuteration on the accuracy of the measurement, we have calculated the transfer efficiency for a proton located far from the interface *e.g.* on the other side on the target (cube) protein (see Fig. S8). This proton, circled in red in Fig. S8, is located 826 pm away from the closest proton of the source (cube) protein. For the HIPRO target protein, after the mixing period of 300 ms, the transfer efficiency for this distant proton is 30 % of the efficiency for the proton at the center of the interface for a 10 ns tumbling-time system, this efficiency increases to 50% when the tumbling time is 20 ns. In a REDPRO system with a 20 ns

tumbling time, the transfer efficiency to the remote proton is only 8 % compared to the proton at the interface. This number drops to 5 % for a system with tumbling time of 10 ns and is below 15 % for a system with tumbling time of 30 ns. The use of a REDPRO labeling scheme is critical if one wants to ensure the accuracy of the determined surface. The use of a fully protonated sample may lead to a better sensitivity but may also lead to a very low level of accuracy in the data.

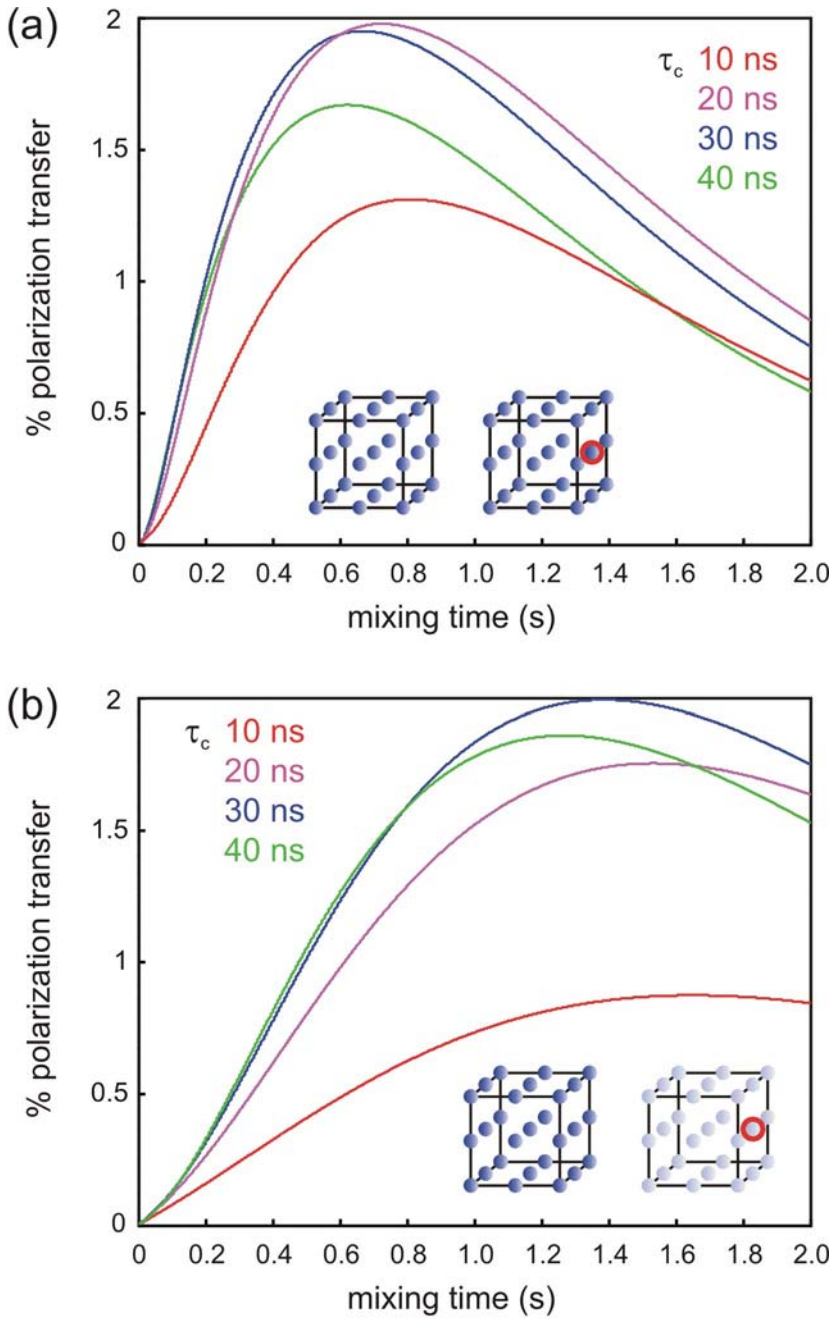
(a)
% polarization transfer
mixing time (s)
τc 10 ns
20 ns
30 ns
40 ns
(b)
% polarization transfer
mixing time (s)
τc 10 ns
20 ns
30 ns
40 ns

Figure S8: The transfer efficiency from the source protein (left cube) to the sphere circled in red in right cube (target protein) is plotted versus the duration of the transfer.

(a) When the target system is HIPRO as represented by dark blue spheres in the right cube and; (b) when the target system has a 10 % proton density as represented by light blue spheres in the right cube. See also legend to Fig. S7.

It may be possible to recover a reasonable accuracy in a protonated sample if one employs mixing times shorter than 100 ms for small tumbling times, (*i.e.* 10 ns and below) even though a REDPRO sample would still show much less spin-diffusion. In this case, the sensitivity drops to the level that is comparable to REDSPRINT. Nevertheless, one can study protein complexes whose tumbling time is less than 10 ns without deuteration as long as the mixing time is kept short.

The efficiency of transfer ε_{ij} from a proton H^i to a proton H^j in a NOESY experiment may be defined as the contribution to the intensity of a cross peak from the first free induction decay recorded, *i.e.* in the absence of any chemical shift evolution in indirect dimensions. In the absence of chemical shift degeneracy, we have:

$$\varepsilon_{ij} = \left\langle H_z^j \left| \exp\left(-\hat{R}\tau_m\right) \right| H_z^i \right\rangle \qquad \text{(S-1)}$$

where $\hat{R}$ is the relaxation matrix and τ_m the mixing time. This quantity can be calculated in a straightforward manner as a selective NOESY experiment.(Zwahlen, Vincent et al. 1994) Figure S9 shows the result for our simplified model of a complex with two fully protonated binding partners.

One can observe that, with increasing size, spin-diffusion affects the efficiency of the transfer at shorter mixing times. Except for smaller systems (τ_c < 15 ns) the maximum efficiency is lower than one per thousand, which is much lower than the efficiency of REDSPRINT. For example for a system with a tumbling time of 20 ns, the transfer efficiency of REDSPRINT after 300 ms is about 5 %. In a selective NOESY experiment, the efficiency after 50 ms is about 0.08 %. Taking into account the low proton density of the target in the REDSPRINT protocol, the transfer efficiency is still greater by a factor of 6. The effect of the efficiency of the HSQC detection and of the line-width in the proton dimension leads to attenuation by a factor of 4 in a protonated sample (*vide supra*). Thus, this leads to an increase of intensity by a factor of 24 in the REDSPRINT experiment.

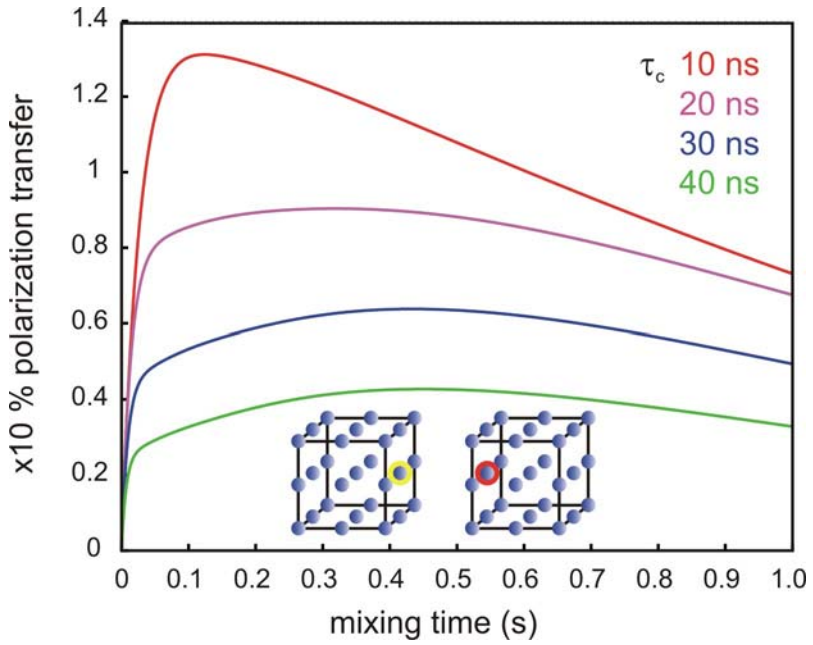

Figure S9: Expectation value of the polarization of the proton circled in red in a selective NOESY experiment.

The definition of the complex system is similar to Figure S7. In the initial state of the simulation, all protons are saturated except the one marked by a yellow circle. The polarization of the latter is attenuated by a factor that takes into account transverse relaxation during the filter.

Conversion of the normalized polarization transfer into the sum of intermolecular NOE's:

In order to obtain an expression that is both reasonably accurate and convenient to use, we have used a simplified model for intermolecular cross-relaxation based on the following hypothesis:

(i) The decay of longitudinal polarization in the source protein is much slower than other processes.

(ii) Intermolecular cross-relaxation is not a dominant process

(iii) Spin-diffusion within the target protein can be described with one neighboring proton

Therefore, we have the following evolution of the longitudinal polarizations:

$$\frac{d}{dt}\begin{pmatrix} S_z \\ I_z \\ I_z^{SD} \end{pmatrix} = \begin{pmatrix} 0 & 0 & 0 \\ \Sigma & -S & S \\ 0 & S & -S \end{pmatrix}\begin{pmatrix} S_z \\ I_z \\ I_z^{SD} \end{pmatrix} \qquad \text{(S-2)}$$

where $\underline{S_z}$ is the source protein polarization, I_z the interface proton from the target protein and I_z^{SD} the polarization of a non-interfacial proton in the target protein. Σ is the sum of intermolecular cross-relaxation rates between the interfacial proton and all protons of the source protein and S is the spin-diffusion rate within the target protein.

With an initial state:

$$\begin{pmatrix} S_z \\ I_z \\ I_z^{SD} \end{pmatrix} = \begin{pmatrix} 1 \\ 0 \\ 0 \end{pmatrix} \qquad \text{(S-3)}$$

The integration of equation S-2 gives equation 1 (main text) for the observable $\langle I_z \rangle(t)$.

A few comments need to be made. The absence of a complete network of cross-relaxation and non-selective relaxation in the target protein leads to an inaccurate description of the polarization after long durations. Nevertheless, equation 1 has been compared to the results presented in Figure 2 and shows a very good level of agreement. In the presence of large intermolecular cross-relaxation, Equation 1 overestimates the expected transfer. This leads to an underestimation of the sum of intermolecular cross-relaxation rates in our analysis, so that the effective intermolecular distances may be slightly overestimated (the error is much reduced due to the distance dependence of dipolar cross-relaxation). A more accurate picture should be obtained by replacing this simple model with a complete calculation, using the CORCEMA approach.(Jayalakshmi and Rama Krishna 2002)

NEBULA results for the Csk SH3-PEP complex in pure ^2H_2O:

NEBULA calculations were carried out on a sample of the Csk SH3-PEP complex. The concentration of Csk SH3 was 450 μM. Other experimental and computational details are equivalent from those employed for the Csk SH3-PEP complex in a mixture of ^2H_2O and [$^2H_8$]glycerol.

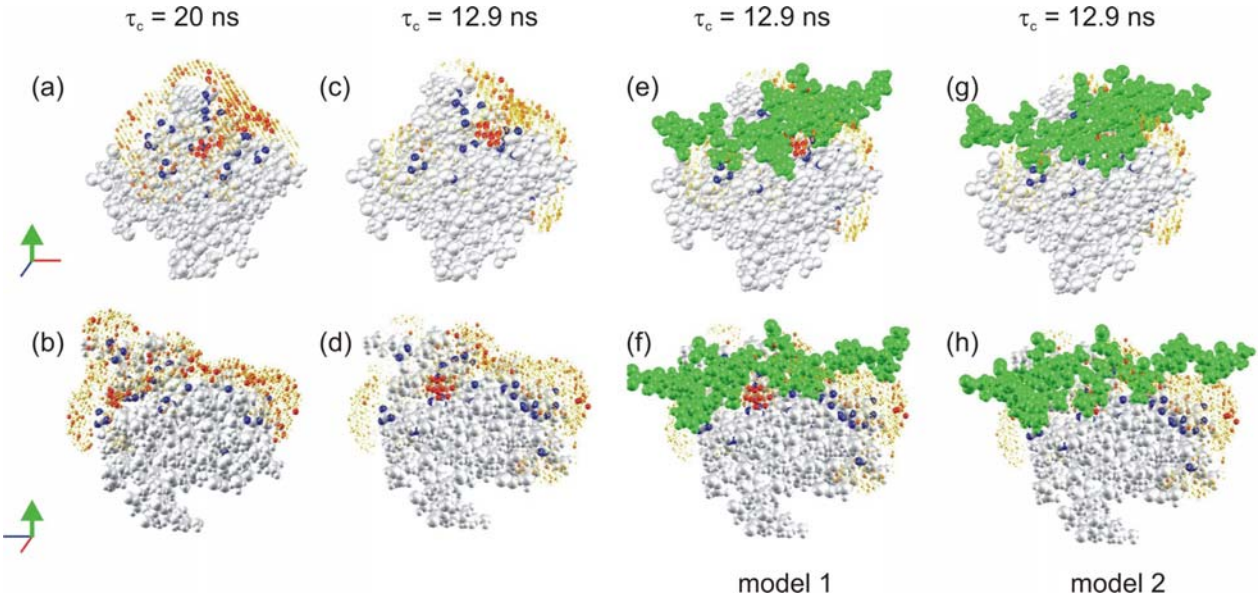

Figure S10: Results of the NEBULA calculations for the Csk SH3-PEP complex in ^2H_2O

and comparison with results in a ^2H_2O/[$^2H_8$] glycerol solution. For detail description please read the legend of Figure 5. (a, b) The NEBULA plot showing the Csk SH3-PEP complex in D_2O/[$^2H_8$]glycerol (Figure 5-e, g). The NEBULA plot showing the Csk SH3-PEP complex in D_2O (c, d), with the PEP obtained from the first model (e, f) and with the PEP obtained from second model (g, h) of the NMR ensemble (PDB code 1JEG).

Overall the NEBULA calculations for the Csk SH3-PEP complex in $^{2}H_2O$ and in a mixture of D_2O/[$^{2}H_8$]glycerol are quite comparable. The small variations in the position of the high proton-density clusters can be attributed to the slight difference in the set of protons that were observed in the two samples.

An interesting feature can be observed in Figures S10 d, f and h. A high proton density cluster appears close to the center of Figure S10d. The first model in the PDB file (1JEG) of the NMR structure of the complex does not fit into this volume (Figure S10f). However, the peptide in the second model of the PDB file shows a different conformation for the side-chain of Arg15 with its side-chain filling the NEBULA cluster (Figure S10h). Note that out of 25 models, 20 show Arg15 in the same orientation as in Figure S10h. Our results support this orientation, illustrating the finer details that REDSPRINT protocol can provide.

Fast mapping of the Csk SH3-PEP complex in a ^2H_2O/[$^2H_8$] glycerol mixture

Figure S11 shows the interface residues appearing on the aliphatic REDSPRINT spectrum. For high molecular weight systems identifying the methyl groups at the interface is quite useful and can be easily done by REDSPRINT approach. In our case we were able to identify (see polarization transfer from PEP to the methyl protons of the Csk SH3 domain) all the methyl groups, which are located at the interface. Unfortunately, the region of the SH3 domain facing the poly-proline part of the peptide ligand does not have any methyl protons, and so we were not able to get a contiguous interacting surface. The aromatic REDSPRINT spectrum had very poor signal intensity and, therefore, interacting residues could not be identified.

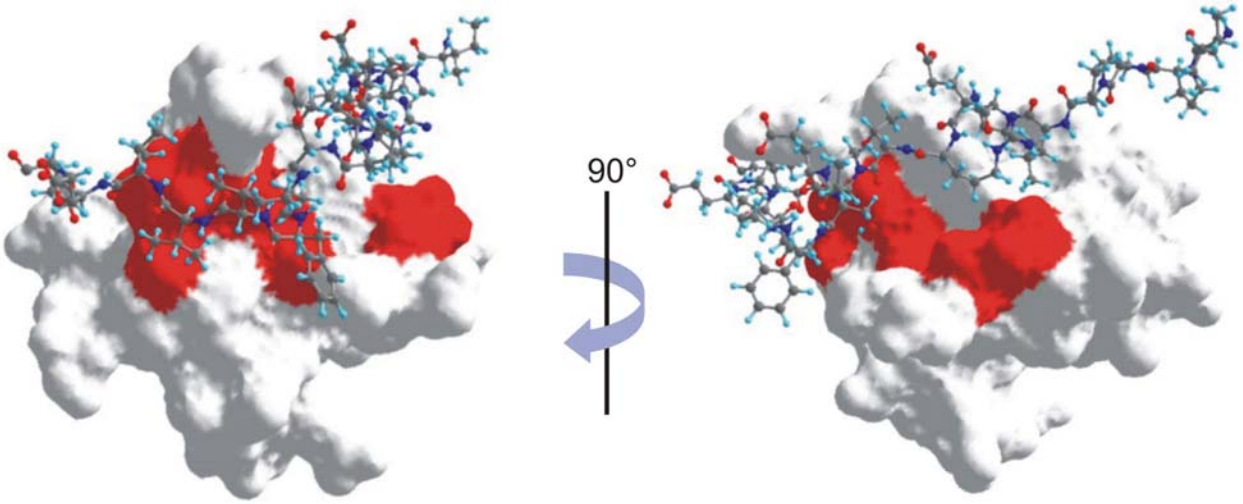

Figure S11: Residues of the Csk SH3 domain identified on the aliphatic REDSPRINT spectrum as part of the interface with PEP are displayed in red. All peaks whose intensity is greater than 35% of the most intense peak were considered to be interacting and thus mapped onto the surface of the Csk SH3 domain. These signals correspond to methyl groups of residues T23, A24, A40, V41, T42 and I59.

Full-page version of the figures:

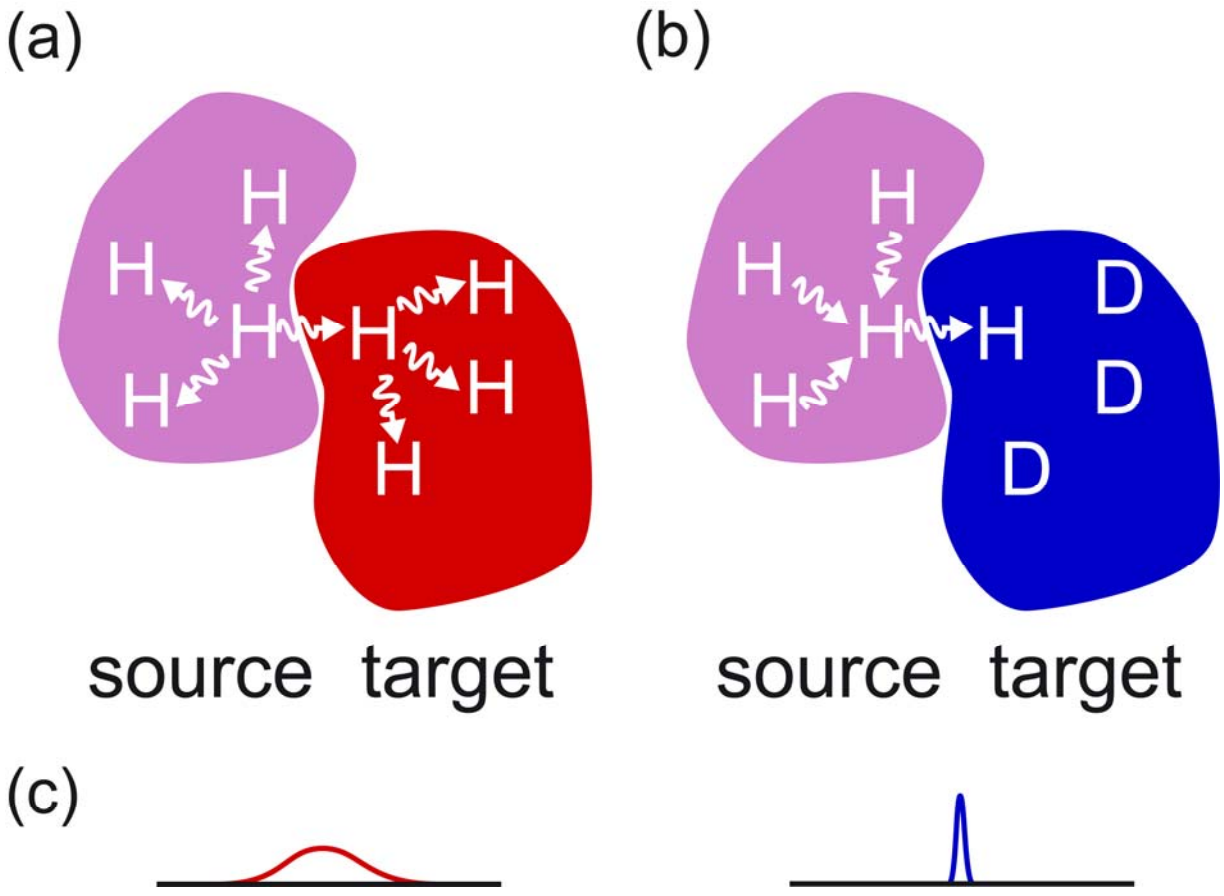

Figure 1

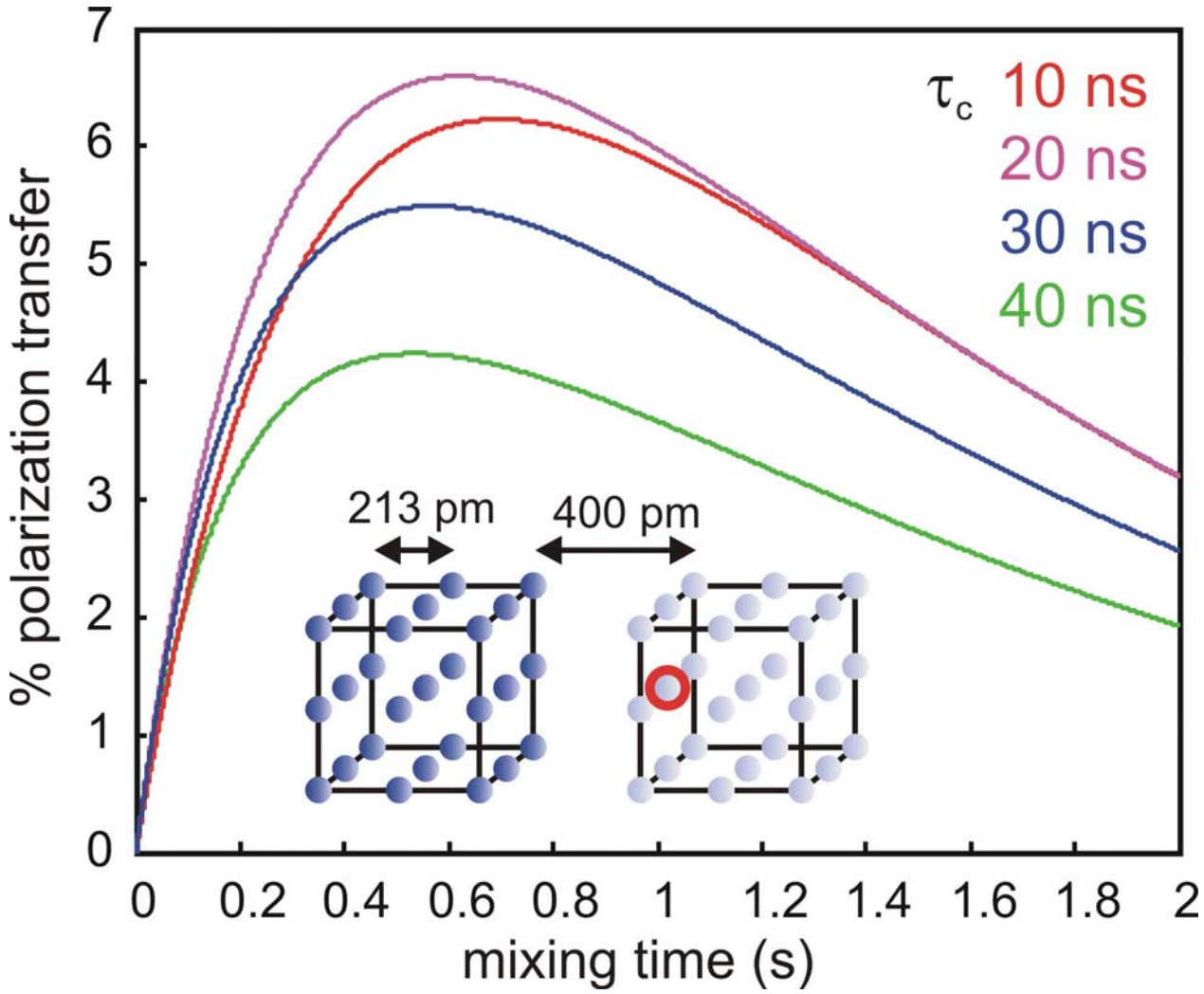
% polarization transfer
mixing time (s)
τc 10 ns
20 ns
30 ns
40 ns
213 pm
400 pm
0
1
2
3
4
5
6
7
0
0.2
0.4
0.6
0.8
1
1.2
1.4
1.6
1.8
2

Figure 2

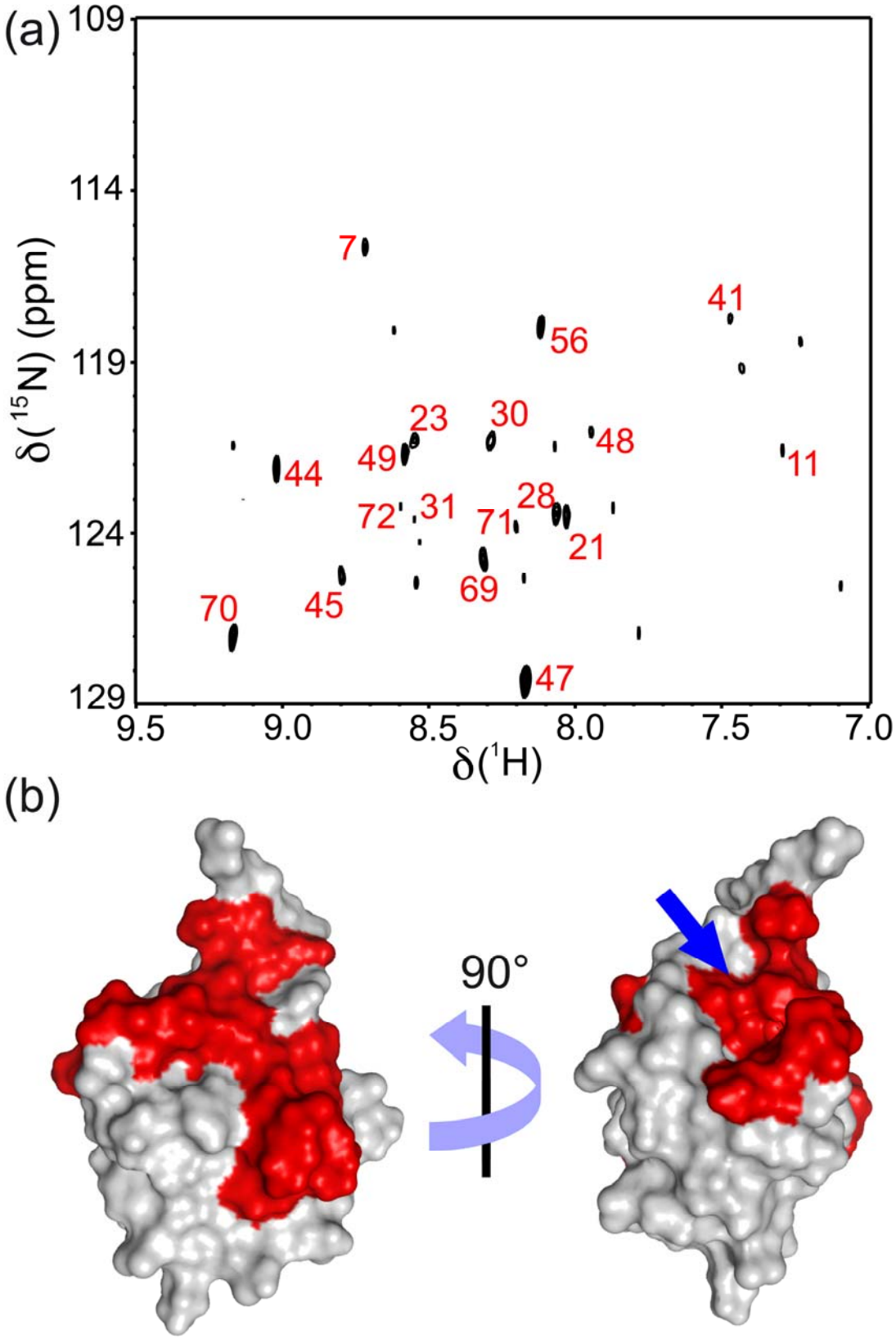
(a)
109
114
119
124
129
δ(15N) (ppm)
9.5
9.0
8.5
8.0
7.5
7.0
δ(1H)
7
41
56
23
30
48
49
44
11
72
31
28
71
21
69
70
45
47
(b)
90°

Figure 3

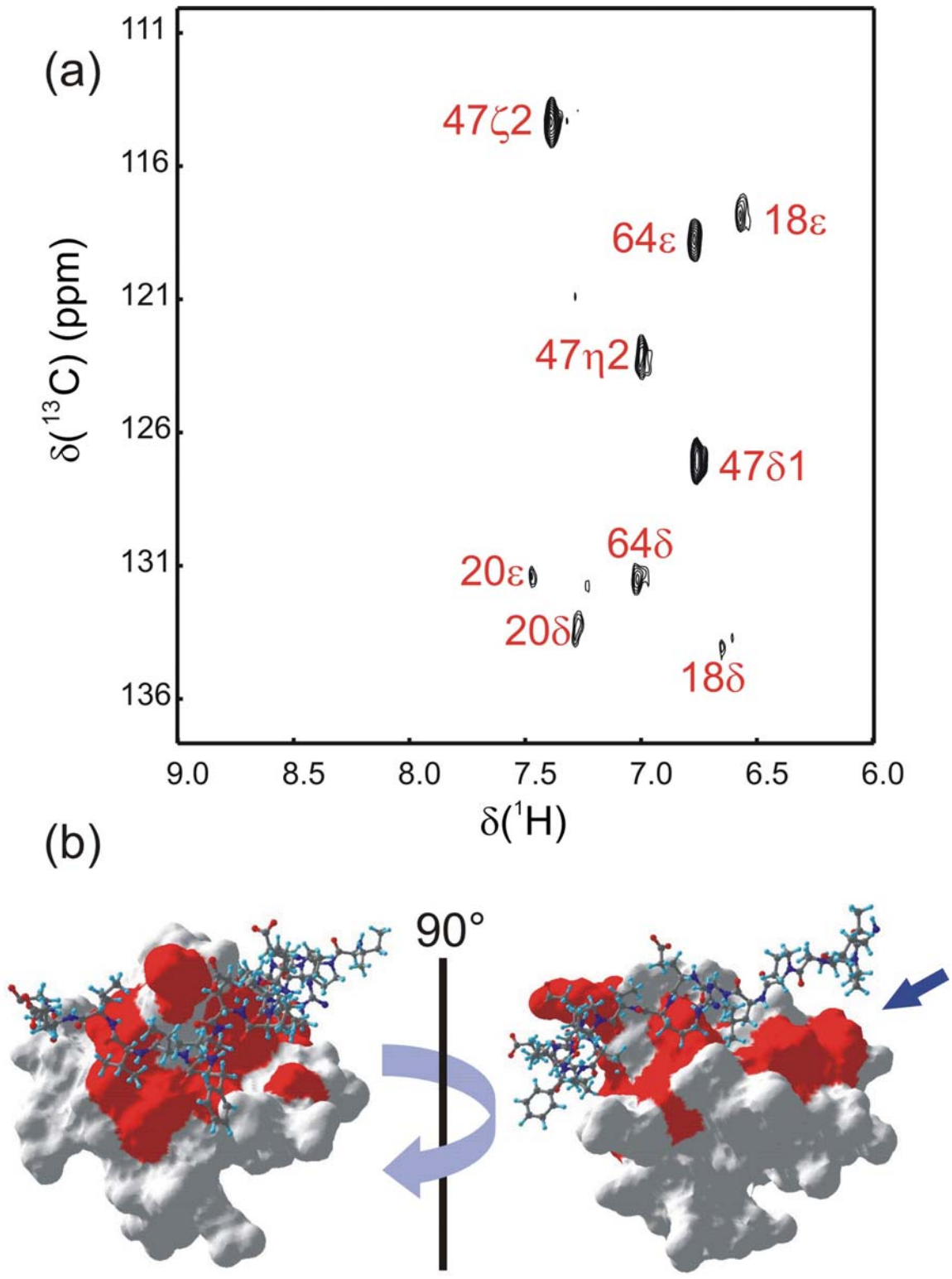
(a)
47ζ2
18ε
64ε
47η2
47δ1
64δ
20ε
20δ
18δ
δ(13C) (ppm)
δ(1H)
111
116
121
126
131
136
9.0
8.5
8.0
7.5
7.0
6.5
6.0
(b)
90°

Figure 4

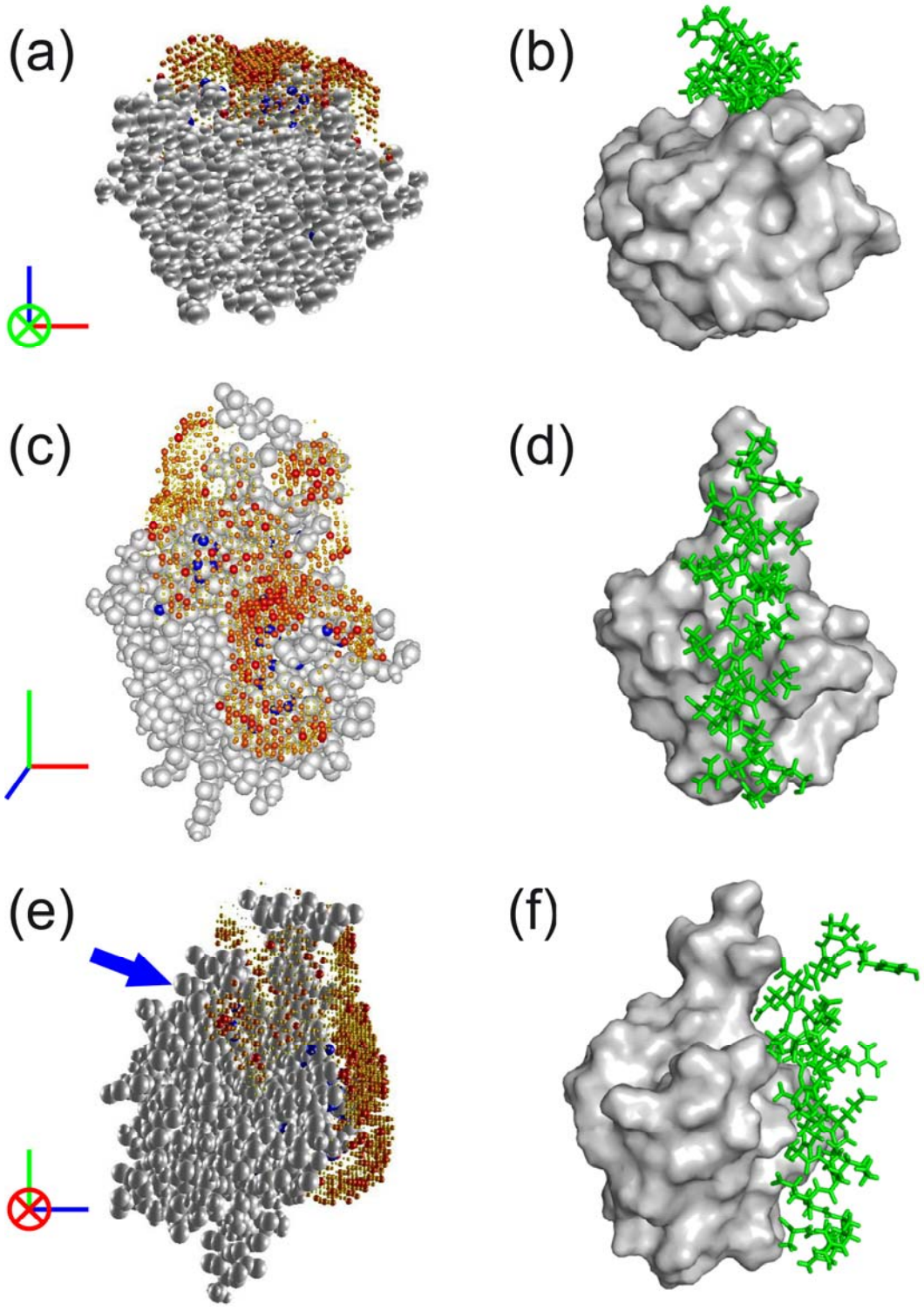

Figure 5

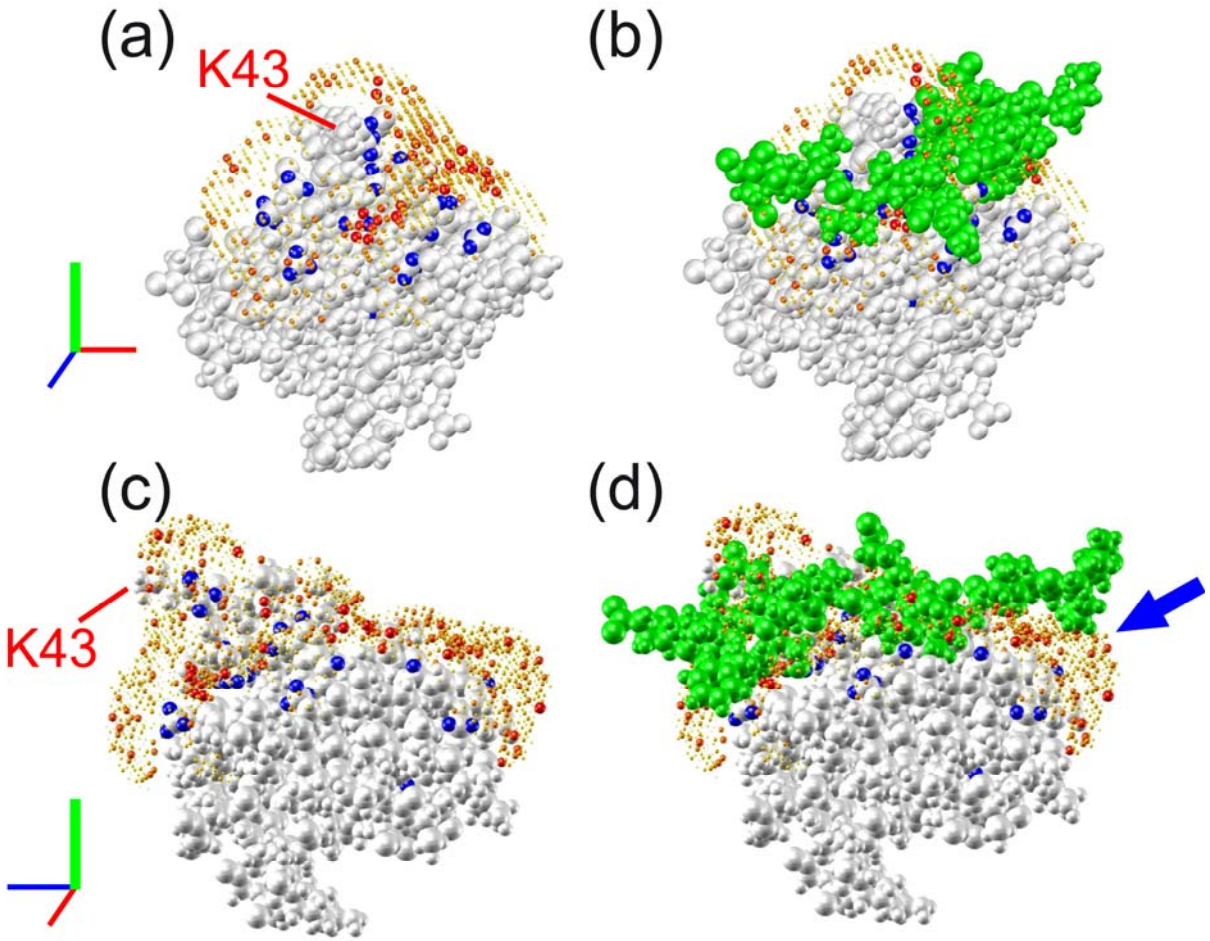

Figure 6

Listing of MATLAB program for generation of NEBULA results

```
%% intitiate variables specific to this demo

clear
randn('state',1);   % defined random number sequence


file='1JEG-SH3.pdb';
constraints_file='constraints_renorm_20ns.csv';
tauc = 20;  % estimate of tau c in ns
tm = 0.3;     % mixing time in seconds
n_mc = 2000000 ; % number of MC sims
noe_cutoff = 0.20 ;    % cutoff of the normalized transfer

%% load a pdb file
[aname, t_aname, anum, resnam, t_resnam, resnum, ...
   coord, b, cards]= own_getpdb(file); % this uses the internal getpdb at NYSBC
constraints=load(constraints_file) ;

%% Interface.m source
%calculates the interface in a complex with unassigned cross-relaxation
%data
%first load pdb file with getpdb
%load constraint file as constraints
%set dynamics parameters

%sets number of atoms with constraint
n_ci=size(constraints);
n_c=n_ci(1);
%sets number of groups of equivalent atoms with constraints
n_cj=max(constraints);
n_g=n_cj(2);

%% calculates basic relaxation constants to be used afterwards and conversion
%of normalized polarization  transfer to sum of the NOE's
% expressions from Art Palmer's book
w0=2*pi*500.13*10^6;
d00=1*(1.05457)*(26.7522)^4*10^6;
% r will be in angstroms!
% tauc=input('what is the estimate of tauC (in ns)?')
%tm=input('what is the mixing time (in s)?')
tc=tauc/10^9;
```

```
te=10/10^12;
s2=1;%0.7;
%[j0,j1,j2] = J_mf(tc,s2,te,w0);
t=te*tc/(te+tc);
j0=2/5*(s2*tc)+(1-s2)*t;
j1=2/5*(s2*tc/(1+(w0*tc)^2)+(1-s2)*t/(1+(w0*t)^2));
j2=2/5*(s2*tc/(1+(2*w0*tc)^2)+(1-s2)*t/(1+(2*w0*t)^2));

Sig0=d00/4*(6*j2-j0);
r1hh=d00/4*(j0+3*j1+6*j2);
r2hh=d00/8*(5*j0+9*j1+6*j2);
SD=tauc/5;
LAMBDA=tm*(1/2+(1-exp(-2*SD*tm))/(4*SD*tm)); %LAMBDA=tm*(1/2+(1-exp(-
2*SD*tm))/(4*SD*tm));

%% makes a table with masses corresponding to t_aname entries
n_ai=size(t_aname);
n_a=n_ai(1);
t_mass=zeros(n_a,2);

for i=1:1:n_a
   l=0;
   while l==0
      j=1;
      while j+5*l<5
         if t_aname(i,j)=='H',
            m_i=1;
            el_i='H';
            l=1;
            j=5;
         else
            j=j+1;
         end
      end
      j=1;
      while j+5*l<5
         if t_aname(i,j)=='C',
            m_i=13;
            el_i='C';
            l=1;
            j=5;
         else
            j=j+1;
         end
      end
      j=1;
      while j+5*l<5
```

```
        if t_aname(i,j)=='N',
            m_i=15;
            el_i='N';
            l=1;
            j=5;
        else
            j=j+1;
        end
    end
    j=1;
    while j+5*l<5
        if t_aname(i,j)=='O',
            m_i=16;
            el_i='O';
            l=1;
            j=5;
        else
            j=j+1;
        end
    end
    j=1;
    while j+5*l<5
        if t_aname(i,j)=='S',
            m_i=32;
            el_i='S';
            l=1;
            j=5;
        else
            j=j+1;
        end
    end
  end
  t_mass(i,1)=m_i;
  t_mass(i,2)=el_i;
end

%% then move the origin to the center of mass with   tomedianpoint.
% tomedianpoint;
%to be used with a protein pdb file loaded with getpdb
%moves the origin of the frame to the median point of the structure

n_i=size(anum);
n=n_i(1);

%calculate median point coordinates

dist_max=max(coord);
```

```
dist_min=min(coord);
X=(dist_max(1)+dist_min(1))/2;
Y=(dist_max(2)+dist_min(2))/2;
Z=(dist_max(3)+dist_min(3))/2;

%calculate new coordinates
new_coord=zeros(n,3);
for i=1:1:n
   new_coord(i,1)=coord(i,1)-X;
   new_coord(i,2)=coord(i,2)-Y;
   new_coord(i,3)=coord(i,3)-Z;
end

%calculates dimensions of the spanned space
dist_tocenter=zeros(n,1);
for i=1:1:n
   dist_tocenter(i)=sqrt((new_coord(i,1))^2+(new_coord(i,2))^2+(new_coord(i,3))^2);
end
max(dist_tocenter);
xyz_max=max(new_coord);
xyz_min=min(new_coord);

x_max=round(xyz_max(1))+5;
x_min=round(xyz_min(1))-5;
y_max=round(xyz_max(2))+5;
y_min=round(xyz_min(2))-5;
z_max=round(xyz_max(3))+5;
z_min=round(xyz_min(3))-5;

n_x=x_max-x_min+1;
n_y=y_max-y_min+1;
n_z=z_max-z_min+1;

%number of elements in the 3D array
'number of points in the 3D array'
n_x*n_y*n_z

%atoms from the protein that are within 7 A from the interface
%which_proteinatoms;
k_p=1;
atoms_close=zeros(1,n); % approx dim
dist_p=zeros(n_c,1);

for i_p=1:1:n
   x_atp=new_coord(i_p,1);
   y_atp=new_coord(i_p,2);
   z_atp=new_coord(i_p,3);
```

```
   %dist_p=[];
   for j_p=1:1:n_c
      n_at=constraints(j_p,1);
      x_at=new_coord(n_at,1);
      y_at=new_coord(n_at,2);
      z_at=new_coord(n_at,3);
      dist_p(j_p)=sqrt((x_atp-x_at)^2+(y_atp-y_at)^2+(z_atp-z_at)^2);
   end
   if min(dist_p)<7,
      atoms_close(k_p)=anum(i_p);
      k_p=k_p+1;
   end
end

% resize atoms_close
atoms_close=atoms_close(atoms_close ~= 0 );

n_aci=size(atoms_close);
n_ac=n_aci(2);
'atoms from protein'
n_ac

%space is defined as a 3D array of points
%test_dist: indices = position from corner of cube, value = 1 if within 5 A
%no steric clash and no nOe too high for constraints file, 0 otherwise

test_dist=false(n_x,n_y,n_z); % assume nothing valid to start with
% future - this should probably be redone as a list.  As such, 1) matrix
% dimension is not then important, and probably best to work with an n^3
% cube of positive integers ; 2) best to build against the actual new_coord
% set directly rather than this way.  3) new_coord can be filterd for
% active atoms only before hand

%all_noe=2D array; for positions with a 1 in test_dist, first three columns
%are i, j an k, next n_c columns are the calculated nOe effects

all_noe0=zeros(3*numel(atoms_close),ceil(numel(atoms_close)/4)+1);  %  approx dims
all_noe2=all_noe0;
all_noe1=all_noe0;
all_noe_gi=zeros(1,numel(atoms_close)); %approx dims
protons_close5=all_noe_gi;
k_n=1;

%% setup for vdw for all close atoms
v(1)=1.2;   %H
v(13)=1.7;  %C
v(15)=1.55; %N
```

```
v(16)=1.52;     %O
v(32)=1.8;  %S
vv=v(t_mass(aname(atoms_close),1)); % vector of call vdws
if any (~vv),   % zeros test
   error('vdw table');
end
vtest=(vv+1.2).^2;  % square of test distance

%% atom list

tmps= (new_coord(constraints(:,1),:));
tmpz = new_coord(atoms_close',:);

for i=1:1:n_x
   x= (i-1+x_min);
   for j=1:1:n_y
      y= (j-1+y_min);
      for k=1:1:n_z
         z= (k-1+z_min);
       dist=(x-tmps(:,1)).^2 + (y-tmps(:,2)).^2 + (z-tmps(:,3)).^2;
        % if any ( dist < 25), %.42
        % if min(dist) < 25,  %.51
        for ii=1:n_c,
           if dist (ii) < 25, % comparison of squares , inside the 5
          % A limit
              test_dist(i,j,k)=true; %this code executed once then break
              for m=1:1:n_ac
                 if((x-tmpz(m,1))^2+(y-tmpz(m,2))^2+(z-tmpz(m,3))^2)<= vtest(m) % square
comparison to precalculated limit
                    test_dist(i,j,k)=false;
                    break % m loop
                 end
              end
              if test_dist(i,j,k),
                 for k_g=1:1:n_g
                    k_gi=0;
                    sig=0;

                     for l=1:1:n_c
                      if constraints(l,2)==k_g,
                        sig=sig+Sig0*dist(l).^-3;   % dist is now the square
                        k_gi=k_gi+1;
                      end
                     end
                    all_noe_gi(k_g)=sig/k_gi;
                 end
                 all_noe0(k_n,1)=i;
```

```
                all_noe0(k_n,2)=j;
                all_noe0(k_n,3)=k;
                for l=1:1:n_c
                   k_ni=constraints(l,2);
                   if abs(all_noe_gi(k_ni))<=(constraints(l,3)+constraints(l,4))/LAMBDA,
                      all_noe0(k_n,l+3)=all_noe_gi(k_ni);
                   else
                      test_dist(i,j,k)=false;
                   end
                end

                if test_dist(i,j,k)
                   k_n=k_n+1;
                end
             end
             break % ii
          end

       end
    end
  end
end

numel(find(test_dist))


%% which_proteinprotons
k_p=1;


%  Now all hydrogen sites with a deuteron nucleus are excluded from the
%  constraints analysis (may change depending on the sample)

n_ana_i=size(t_aname);
n_ana=n_ana_i(1);

tmps=cellstr(t_aname);

% which_ha;
t_ha=[find(strcmp(tmps,' HA')) find(strcmp(tmps,'1HA')) find(strcmp(tmps,'2HA'))];
n_ha_i=size(t_ha);
n_ha=n_ha_i(2);

% which_hn;
t_hn=find(strcmp(tmps,' H'))';

%  which_sidechain;
```

```
t_sd=[find(strcmp(tmps,' HG1')) find(strcmp(tmps,'1HZ')) find(strcmp(tmps,'2HZ'))
find(strcmp(tmps,'1HE2')) find(strcmp(tmps,'2HE2')) find(strcmp(tmps, ' HH'))];
n_sd_i=size(t_sd);
n_sd=n_sd_i(2);

% which_hg;
t_hg = find(strcmp(tmps,' HG'))';

%%which_xhd2;
t_xhd2=[find(strcmp(tmps,'1HD2')) find(strcmp(tmps,'2HD2'))];
n_xhd2_i=size(t_xhd2);
n_xhd2=n_xhd2_i(2);

%%which_hd1;
t_hd1=find(strcmp(tmps,' HD1'))';
n_hd1_i=size(t_hd1);
n_hd1=n_hd1_i(2);

% which_he1;
t_he1=find(strcmp(tmps,' HE1'))';
n_he1_i=size(t_he1);
n_he1=n_he1_i(2);

tmps=cellstr(t_resnam);
% which_ser;
t_ser =find(strcmp(tmps,' SER'))';
n_ser_i=size(t_ser);
n_ser=n_ser_i(2);

% which_cys;
t_cys = find(strcmp(tmps,' CYS'))';
n_cys_i=size(t_cys);
n_cys=n_cys_i(2);

%which_asn;
t_asn = find(strcmp(tmps,' ASN'))';
n_asn_i=size(t_asn);
n_asn=n_asn_i(2);

%%which_his;
t_his = find(strcmp(tmps,' HIS'))';
n_his_i=size(t_his);
n_his=n_his_i(2);

% which_trp;
t_trp = find(strcmp(tmps,' TRP'))';
n_trp_i=size(t_trp);
```

```
n_trp=n_trp_i(2);

dist_p5=zeros(1,n_c);
for i_p=1:1:n
   x_atp=new_coord(i_p,1);
   y_atp=new_coord(i_p,2);
   z_atp=new_coord(i_p,3);

   for j_p=1:1:n_c
      n_at=constraints(j_p,1);
      x_at=new_coord(n_at,1);
      y_at=new_coord(n_at,2);
      z_at=new_coord(n_at,3);
      dist_p5(j_p)=sqrt((x_atp-x_at)^2+(y_atp-y_at)^2+(z_atp-z_at)^2);
   end
   if min(dist_p5)<5,
      k_pp=aname(i_p);
      k_ppres=resnam(i_p);
      test_hd=1;
      for k_ha=1:1:n_ha
         t_ha_k=t_ha(k_ha);
         if k_pp==t_ha_k,
            test_hd=0;
         end
      end
      for k_sd=1:1:n_sd
         t_sd_k=t_sd(k_sd);
         if k_pp==t_sd_k,
            test_hd=0;
         end
      end
      if any ( t_hg == k_pp )
         for k_ser=1:1:n_ser
            t_ser_k=t_ser(k_ser);
            if k_ppres==t_ser_k,
               test_hd=0;
            end
         end
         for k_cys=1:1:n_cys
            %t_cys_k=t_ser(k_cys);
            t_cys_k=t_cys(k_cys);
            if k_ppres==t_cys_k,
               test_hd=0;
            end
         end
      end
      for k_xhd2=1:1:n_xhd2
```

```
        t_xhd2_k=t_xhd2(k_xhd2);
        if k_pp==t_xhd2_k,
          for k_asn=1:1:n_asn
            t_asn_k=t_asn(k_asn);
            if k_ppres==t_asn_k,
              test_hd=0;
            end
          end
        end
      end
      for k_hd1=1:1:n_hd1
        t_hd1_k=t_hd1(k_hd1);
        if k_pp==t_hd1_k,
          for k_his=1:1:n_his
            t_his_k=t_his(k_his);
            if k_ppres==t_his_k,
              test_hd=0;
            end
          end
        end
      end
      for k_he1=1:1:n_he1
        t_he1_k=t_he1(k_he1);
        if k_pp==t_he1_k,
          for k_trp=1:1:n_trp
            t_trp_k=t_trp(k_trp);
            if k_ppres==t_trp_k,
              test_hd=0;
            end
          end
        end
      end
      if any ( k_pp==t_hn)
        test_hd=0;
      end
      if test_hd==1,
        prot=t_mass(k_pp,1);
        if prot==1,
          protons_close5(k_p)=anum(i_p);
          k_p=k_p+1;
        end
      end
    end
end

%% close protons examined
protons_close5=protons_close5(protons_close5 ~= 0 );
```

```
n_ppi=size(protons_close5);
n_pp=n_ppi(2);
k_pp=1;
for mijk=1:1:k_n-1
   all_noe2(mijk,1)=all_noe0(mijk,1);
   all_noe2(mijk,2)=all_noe0(mijk,2);
   all_noe2(mijk,3)=all_noe0(mijk,3);
end
for m=1:1:n_pp
   i_m=protons_close5(m);
   if k_pp<=n_c,
      if i_m==constraints(k_pp,1),
         for m_p=1:1:k_n-1
            all_noe2(m_p,m+3)=all_noe0(m_p,k_pp+3);
         end
         k_pp=k_pp+1;
      else
         x_pt=new_coord(i_m,1);
         y_pt=new_coord(i_m,2);
         z_pt=new_coord(i_m,3);
         for m_p=1:1:k_n-1
            x_atm=all_noe0(m_p,1)-1+x_min;
            y_atm=all_noe0(m_p,2)-1+y_min;
            z_atm=all_noe0(m_p,3)-1+z_min;
            dist_prot= ((x_pt-x_atm)^2+(y_pt-y_atm)^2+(z_pt-z_atm)^2);  % square used
            all_noe2(m_p,m+3)=Sig0/dist_prot.^3;    % note square dist
         end
      end
   else
      x_pt=new_coord(i_m,1);
      y_pt=new_coord(i_m,2);
      z_pt=new_coord(i_m,3);
      for m_p=1:1:k_n-1
         x_atm=all_noe0(m_p,1)-1+x_min;
         y_atm=all_noe0(m_p,2)-1+y_min;
         z_atm=all_noe0(m_p,3)-1+z_min;
         dist_prot= ((x_pt-x_atm)^2+(y_pt-y_atm)^2+(z_pt-z_atm)^2);
         sig=Sig0/dist_prot.^3;  % square used
         all_noe2(m_p,m+3)=sig;
      end
   end
end

if k_pp~=n_c+1,
   'error in building of all_noe2'
end
```

```
%% montecarlo

%% resize  all_noe0 to ctual used values
all_noe0=all_noe0(all_noe0(:,1) > 0 , : );

all_noe2=all_noe2(all_noe2(:,1) > 0 , : );

n_pi=size(all_noe0);
n_p=n_pi(1);
config=false( n_p,1);
results=false(min(ceil(n_mc/32)+1,50  ) , n_p);     % CARE TO TRUNCATE!
energies=[];
k_mc=1;
energy0=1.5^2*n_p;
noe_exp=zeros(1,n_pp);
noe_err=noe_exp;
k_pi=1;


%% choose the density of sites in the NEBULA occupied by protons:
%correspondance between values of A and density:
%-1.754=0.04, -1.647=0.05, -1.598=0.055, -1.557=0.06, -1.476=0.07,
%-1.405=0.08, -1.341=0.09, -1.282=0.10
A=-1.476;%-1.476;
% 1/2*(1+erf(A/sqrt(2)))

tic
%% filter out constraints assigned to burried residues:
constraints2=constraints;

dist_cons=zeros(k_n-1,1);

for m_t=1:1:n_c
   i_t=constraints(m_t,1);
   x_pt=new_coord(i_t,1);
   y_pt=new_coord(i_t,2);
   z_pt=new_coord(i_t,3);

   for m_p=1:1:k_n-1
      x_atm=all_noe0(m_p,1)-1+x_min;
      y_atm=all_noe0(m_p,2)-1+y_min;
      z_atm=all_noe0(m_p,3)-1+z_min;
      dist_cons(m_p)= ((x_pt-x_atm)^2+(y_pt-y_atm)^2+(z_pt-z_atm)^2);
   end
   if min(dist_cons)>25,   % square used, distance is 5 Ang test
      constraints2(m_t,3)=0;
```

```
   end
end

for m=1:1:n_pp
   m_i=protons_close5(m);
   if k_pi<=n_c,
      if m_i==constraints2(k_pi,1),
         noe_exp(m)=-constraints2(k_pi,3)/LAMBDA;
         if constraints2(k_pi,3)==0,
            noe_err(m)=noe_cutoff/(1.5*LAMBDA);
         else
            noe_err(m)=constraints2(k_pi,4)/LAMBDA;
         end
         k_pi=k_pi+1;
      else
         noe_exp(m)=0;
         noe_err(m)=noe_cutoff/(1.5*LAMBDA);
      end
   else
      noe_exp(m)=0;
      noe_err(m)=noe_cutoff/(1.5*LAMBDA);
   end
end


drawnow;

for l=1:1:n_pp
   all_noe1(1:n_p,l)=all_noe2(1:n_p,l+3);
end

all_noe1= single  (all_noe1(all_noe0(:,1) > 0 , : )); % single spec reduces cost of multiply for
noe_calc, indexed to noe0

%try single, prev exec >.2 s
noe_exp=single(noe_exp);     noe_err=single(noe_err);

for i=1:1:n_mc
   %table=A+randn(n_p,1);   % vector only needed here .
   config =  A+randn(n_p,1)  > 0;
   noe_calc= all_noe1'*single(config) ; % all_noe1 is single, and so is config.  Compute the rest
single precision for size issues.
   energy=single(0);
   for k=1:1:n_pp
      if noe_exp(k)==0,
         energy=energy+((noe_exp(k)-noe_calc(k))).^2/((noe_err(k)).^2);
      else
```

```
        energy=energy+((noe_exp(k)-noe_calc(k))).^2/((noe_err(k)).^2);
      end
   end
   if energy<=energy0,
      for j=1:1:n_p
         results(k_mc,j)=config(j);
      end
      energies(k_mc)=energy;
      k_mc=k_mc+1;
   end
end

tmpt=find(any(results'));
results=results(tmpt,:);


toc

dlmwrite('energies.csv', energies, ' ');
dlmwrite('config_results.csv', results, ' ');

'montecarlo is done'
[a,b]=find(results);
energies  , chksmrw(results)    % test outputs for comparison
```

Liouvillian formalism for the initial linear regime and the equilibrium polarization.

In the framework of a Homogeneous Master Equation (Jeener 1982) (HME), we define the Liouvillian operator that drives the longitudinal relaxation as

$$\left\{E, I_z^1, \ldots, I_z^i, \ldots, I_z^n\right\},$$

where E is the identity operator, I_z^i the longitudinal polarization of proton I^i, and n the number of protons defined in the model. The HME may be written as:

$$\frac{d}{dt}\sigma(t) = -\hat{L}\sigma(t), \qquad \text{(S-4)}$$

$\hat{L}$ is the sum of the relaxation matrix $\hat{\Gamma}$ and the thermal correction $\hat{\Theta}$ (which is defined in equation 5 and 6) terms.(Levitt and Di Bari 1992; Ghose 2000)

Let us first evaluate the terms in the relaxation matrix $\hat{\Gamma}$. The polarization that is transferred from site *j* to *i* is proportional to the average polarization of site *j* and to the probability P_i of finding a proton in site *i*. Neglecting the thermal correction factor, the rate of longitudinal polarization for site *i* is given below:

$$\frac{d\left\langle I_z^i \right\rangle}{dt} = P_i \sum_{j \neq i} \sigma_{ij}^0 \left\langle I_z^j \right\rangle - \sum_{j \neq i} P_j \left(\sigma_{ji}^0 + \rho_{ji}^0\right) \left\langle I_z^i \right\rangle , \quad \text{(S-5)}$$

σ_{ij}^0 and ρ_{ij}^0 are the cross-relaxation and non-selective relaxation rates, respectively, which are determined by the dipole-dipole couplings(Abragam 1961; Cavanagh, Fairbrother et al. 1996) between protons in sites *i* and *j*. They are defined as:

$$\sigma_{ij}^0 = \frac{d_{ij}^2}{4}\left(J_{ij}(0) - 6J_{ij}(2\omega_0)\right) , \quad \text{(S-6A}$$

and,

$$\rho_{ij}^0 = \frac{3d_{ij}^2}{4}\left(J_{ij}(\omega_0) + 4J_{ij}(2\omega_0)\right) , \quad \text{(S-6b)}$$

where $d_{ij} = (\mu_0/4\pi)\hbar\gamma_H^2 r_{ij}^{-3}$, μ_0 is the permeability of free space, $\hbar$ Planck's constant divided by 2π, γ_H the proton gyromagnetic ratio, r_{ij} the average distance between the two proton sites, ω_0 the proton Larmor frequency and $J_{ij}(\omega)$ the spectral density function that describes the motions of the internuclear vector **r**(H_iH_j) at the frequency ω, assuming that the internuclear distance is constant. The following model-free spectral density function(Lipari and Szabo 1982) was used:

$$J_{ij}(\omega) = \frac{2}{5}\left(\frac{S_{ij}^2 \tau_c}{1+(\omega\tau_c)^2} + \frac{\left(1-S_{ij}^2\right)\tau_{ij}}{1+(\omega\tau_{ij})^2}\right) , \quad \text{(S-7)}$$

where $\tau_{ij}^{-1} = \tau_c^{-1} + \tau_{e,ij}^{-1}$, τ_c is the global rotational correlation time (with the assumption of isotropic global tumbling), $\tau_{e,ij}$ is the effective local rotation correlation time, and S_{ij}^2 is the local order parameter describing the mobility of the vector **r**(H_iH_j).

The thermal correction term can be expressed as: (Levitt and Di Bari 1992; Ghose 2000)

$$\theta_{i1} = -\sum_{j=2}^{n+1} \hat{\Gamma}_{ij} \left\langle I_z^{j-1} \right\rangle^{eq} . \quad \text{(S-8)}$$

where $\left\langle I_z^i \right\rangle^{eq}$ is the expectation value of the longitudinal polarization of proton *i* at thermal equilibrium. By normalizing the polarizations(Levante and Ernst 1995), $\left\langle I_z^i \right\rangle^{eq} = P_i$, one obtains the following thermal correction terms:

$$\theta_{i1} = -\sum_{j=2}^{n+1} \hat{\Gamma}_{ij} P_{j-1} . \quad \text{(S-9)}$$

REFERENCES (Supplementary Material):

Abragam, A. (1961). Principles of Nuclear Magnetism. Oxford, Oxford University Press.

Bohlen, J. M. and G. Bodenhausen (1993). "Experimental Aspects of Chirp Nmr-Spectroscopy." J. Magn. Reson. A **102**(3): 293-301.

Cavanagh, J., W. J. Fairbrother, et al. (1996). Protein NMR Spectroscopy: Principles and practice. New York, Academic Press.

Ghose, R. (2000). "Average Liouvillian theory in nuclear magnetic resonance - Principles, properties, and applications." Concepts in Magnetic Resonance **12**(3): 152-172.

Jayalakshmi, V. and N. R. Krishna (2002). "Complete relaxation and conformational exchange matrix (CORCEMA) analysis of intermolecular saturation transfer effects in reversibly forming ligand-receptor complexes." J Magn Reson **155**(1): 106-18.

Jayalakshmi, V. and N. Rama Krishna (2002). "Complete Relaxation and Conformational Exchange Matrix (CORCEMA) Analysis of Intermolecular Saturation Transfer Effects in Reversibly Forming Ligand–Receptor Complexes." J. Magn. Reson. **155**: 106-118.

Jeener, J. (1982). "Superoperators in Magnetic-Resonance." Advances in Magnetic Resonance **10**: 1-51.

Kupce, E., J. Boyd, et al. (1995). "Short Selective Pulses for Biochemical Applications." Journal of Magnetic Resonance Series B **106**(3): 300-303.

Levante, T. O. and R. R. Ernst (1995). "Homogeneous Versus Inhomogeneous Quantum-Mechanical Master-Equations." Chemical Physics Letters **241**(1-2): 73-78.

Levitt, M. H. and L. Di Bari (1992). "Steady state in magnetic resonance pulse experiments." Phys Rev Lett **69**(21): 3124-3127.

Lipari, G. and A. Szabo (1982). "Model-free approach to the interpretation of nuclear magnetic resonance relaxation in macromolecules. 1. Theory and range of validity." J.Amer.Chem.Soc. **104** 4546-4559.

Sklenar, V. and A. Bax (1987). "Spin-Echo Water Suppression for the Generation of Pure-Phase Two-Dimensional Nmr-Spectra." Journal of Magnetic Resonance **74**(3): 469-479.

Zwahlen, C., P. Legault, et al. (1997). "Methods for measurement of intermolecular NOEs by multinuclear NMR spectroscopy: Application to a bacteriophage lambda N-peptide/boxB RNA complex." Journal of the American Chemical Society **119**(29): 6711-6721.

Zwahlen, C., S. J. F. Vincent, et al. (1994). "Quenching Spin-Diffusion in Selective Measurements of Transient Overhauser Effects in Nuclear-Magnetic-Resonance - Applications to Oligonucleotides." J. Am. Chem. Soc. **116**(1): 362-368.